MINISTRY OF EDUCATION AND SCIENCE OF UKRAINE
ODESSA STATE ENVIRONMENTAL UNIVERSITY

A.V. Glushkov, O.Y. Khetselius

MATHEMATICAL PHYSICS OF CLASSICAL AND QUANTUM SYSTEMS. P.7

Lectures Notes

Odesa
Odessa State Environmental University
2023

UDK 539.184:539.27
G41

Glushkov A.V., Khetselius O.Y.
G41 Mathematical Physics of Classical and Quantum Systems.P.7: Lecture's Notes.
Odesa:
Odessa State Environmental University, 2023. 90p.
ISBN 978-966-186-229-5

The book presents the detailed explanation of such topics as as electron-beta-nuclear spectroscopy of atoms and molecules, the effect of the chemical environment on the parameters of beta decay, basic methods in the theory of beta decay and co-operative electron-beta-kaon-nuclear processes, theoretical models of electron rearrangement, induced by nuclear transmutation, the theory of the influence of the chemical environment on the parameters of beta decay, etc.

It can be used by PhD students (postgraduates and scientific workers) of the speciality 113-"Applied Mathematics", as well as 111-"Mathematics" and so on.

UDK 539.184:539.27

Recommended by the Methodical Council of the Odessa State Environmental University of the Ministry of Education and Science of Ukraine as lectures notes (protocol No.2 of 26.10.2022)

ISBN 978-966-186-229-5

CONTENTS

LIST OF ABBREVIATIONS, CONSTANTS, UNITS USED

MPR – multiphoton resonance (1.resonances)
DE – differential equation (1.method)
QED – quantum electrodynamic
LR – laser radiation
REF – relativistic energy formalism
RHF – relativistic approximation Hartree-Fok
PT – perturbation theory
PTDF – many-particle PT with DF zero approximation;
GF – Green's function (1.method)
AC – alternating current
DF – Dirac-Fock (1.method)
DKS – Dirac-Kohn-Sham (1.method)
DC – direct current
LE – Lyapunov's exponents
QP – quasi-particle
XC (1.effects) – exchange-correlation (1.effects)
WKB – WKB approximation

CONSTANTS, UNITS USED

Fundamental constants:

Speed of light c=2,997925·10^{8} м/с; Elementary charge e=1,60219·10^{-19} Кл;
Electron mass m=9,1095·10^{-31} кг; Planck constant $\hbar$=1,05459·10^{-34}Дж·с;
Rydberg constant R_{∞}=1,0973732·10^{7}м$^{-1}$ Bore radius $\hbar^2/me^2$=0,5291773 Å;
Fine-structure constant $\alpha=e^2/\hbar c, 1/\alpha$=137,03597;

Units. Everywhere where otherwise indicated, atomic units are used: e=1, $\hbar$=1, m=1 (1.c=137,03597). Atomic units of length, time and velocity: $\hbar^2/me^2$=5,291773·10^{-11} m, $\hbar^3/me^4$=2,4189·10^{-17} s, $e^2/\hbar$=2,1877·10^{6} m/s. Atomic unit of energy (1.a.u.e.) $me^4/\hbar^2$=2Ry=27,2116eV=4,3598·10^{-18}J=2,19475·10^{5}cm^{-1} (1.$me^4/2\hbar^2$= Ry – Rydberg). Energy in Coulomb unts (1.c.u.): 1 c.u.e.=Z^2 a.u.e. (1.Z – charge of atomic nucleus). Relativistic units: $\hbar$=1, c=1, m=1, e^2=1/137,03597.

Introduction

The discipline "Mathematical Physics of Classical and Quantum Systems" is an important, mandatory discipline in the cycle of professional training of graduate students (1.third level of education) in the specialty 113- Applied Mathematics.

The purpose of studying the discipline is to master (1.provide) a number of competencies, in particular, including the study of modern mathematical physics of classical and quantum systems, to develop and use new mathematical approaches, to build fundamentally new methods and algorithms for systems analysis, mathematical modeling, programming and forecasting in solving current problems of theory and practice of complex classical and quantum systems, in general complex systems, use modern scientific methods and achieve scientific results that create new knowledge.

The place of the discipline in the structural and logical scheme of its teaching: the knowledge gained in the study of this discipline is used in writing dissertations, the subject of which is related to the study of fundamental energy (1.radiation) characteristics of complex classical and quantum systems with possible generalization to various classes of mathematical chemical, cybernetic and other systems.

The basic concepts of the discipline are the desired tools of an experienced specialist in the field of applied mathematics.

After mastering this discipline, the graduate student must be able to use modern or develop new approaches, in particular, based on the apparatus of mathematical physics of classical and quantum systems to analyse, model, predict, program the characteristics of complex classical and quantum systems with computer experiments.

In the lecture’s notes I present a consistent relativistic approach to calculation of energy and spectral parameters of the kaonic exotic atomic systems with accounting for the nuclear radiative (1.quantum electrodynamics), hyperfine and strong interactions. The approach is naturally based on using the relativistic Klein-Gordon-Fock equation with introduction of electromagnetic and strong interactions potentials

PART 1 ELECTRON-B-NUCLEAR SPECTROSCOPY OF ATOMIC SYSTEMS AND MANY-BODY PERTURBATION THEORY APPROACH TO COMPUTING B-DECAY PARAMETERS

Abstract. The modern concepts of physical nature of a beta-decay are briefly presented as well as the main characteristics of a beta-decay, classification of the beta-transitions, selection rules etc. It is presented a new relativistic approach to calculating the characteristics of the β-decay of atomic systems (nuclei), based on the combined relativistic nuclear model and relativistic many-body perturbation theory formalism with correct accounting for exchange-correlation, nuclear, radiation corrections. A relativeistic many-body perturbation theory is applied to electron subsystem, and a nuclear relativistic middle-field model is used for nuclear subsystem. All correlation corrections of the second order and dominated classes of the higher orders diagrams are taken into account. Within the framework of the presented theory, the characteristics of a whole series of allowed (super-allowed) β-decays are calculated, namely, for $^{33}P \rightarrow ^{33}S$, $^{35}S \rightarrow ^{35}Cl$, $^{45}Ca \rightarrow ^{45}Sc$, $^{63}Ni \rightarrow ^{63}Cu$, $^{106}Ru \rightarrow ^{106}Rh$, $^{155}Eu \rightarrow ^{155}Gd$, $^{241}Pu \rightarrow ^{241}Am$ decays. The effect of the chemical environment of an atom on the characteristics (integral Fermi function, half-life) of the beta-transitions is studied. The results of accurate calculation of the beta-decay parameters are presented and compared with alternative theoretical data. Results of computing the Fermi function of a β^--decay with different definitions of this function are presented. The effect of an atomic field type choice on the beta decay characteristics as well as the influence of accounting for the exchange-correlation effects in the wave functions of the discrete and continuous spectrum on the values of the Fermi and integral Fermi functions are calculated. The obtained data are analyzed and compared with available in literature.

Keywords: Beta-decay – Electron-beta-Nuclear Spectroscopy - Relativistic perturbation theory – Correlation, nuclear, radiative corrections - integral Fermi function

1.1 Modern concepts of the physical nature of nuclear beta decay

Nuclear β–decay is a manifestation of the fundamental weak interaction of elementary particles (see, for example, [1-22]). Nuclear β-decay is a manifestation of the fundamental weak interaction of elementary particles (see, for example, [1-6]).

According to modern concepts, beta decay is due to the transformations of quarks: in β^--decay, one d-quark of a nucleon turns into a u-quark, in β^+-decay reverse transformation occurs. The main quanta of the weak interaction are the so-called intermediate bosons – particles of large mass: 81,8 ($W^{\pm}$) 91,2 (Z^0) GeV/s^2. They were opened in 1983 in CERN (European Center for Nuclear Research, Switzerland). The weak interaction due to the large values of the masses of the virtual intermediate bosons $W^{\pm}$ and Z^0 is essentially short-range. It is easy to estimate the radius R of the action of exchange forces, which is characterized by the time (unobservability) Δt of violation of the energy conservation law by the amount of energy $\Delta E = mc^2$ carrier of all types of interactions between particles – virtual boson:

$$R \cong c \cdot \Delta t \cong c \cdot \frac{\hbar}{\Delta E} = \frac{\hbar}{mc}, \qquad (1)$$

where the conjugate parameters Δt and ΔE are related and determined by the Heisenberg uncertainty relation and c is the velocity of light. Hence, the radius of action of weak forces is

$$R_{W,Z} = \frac{\hbar c}{M_{W,Z} \cdot c^2} \cong \frac{200\ MeV \cdot Fm}{100 \cdot 10^3\ MeV} \cong 2 \cdot 10^{-3}\ Fm, \qquad (2)$$

where $\Delta E \approx M_W c^2 \approx M_Z c^2 \approx 100$ GeV.

Weak interaction is the only interaction in which both the electrical charge of fermions and their aroma can change. The change in the charge of fermions is due to the presence of an electric charge in the quanta of the $W^{\pm}$ field. The classical theory of weak interaction considered only processes with a change in charge, such as β- and μ-decays (Figure 1).

As mentioned above, in the modern Weinberg-Glashow-Salam theory of weak interaction, which combines weak and electromagnetic interactions, in addition to charged W-bosons, there is also a neutral Z^0-boson. This corresponds to the course of processes in which the electric charge of fermions does not change. Naturally, here we are talking about neutral currents, which make a contribution, for example, to $\nu_e e$-scattering (Figure 2).

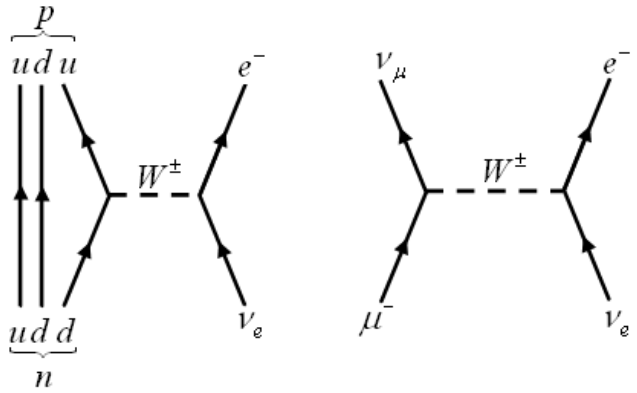

Figure 1 – Feynman diagrams for β- and μ-decays

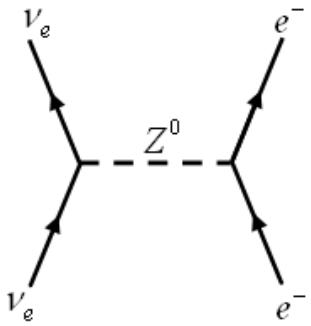

Figure 2 – Contribution of neutral currents to $\nu_e e$-scattering

β-decay of nuclei is one of the three main types of radioactivity. With electronic (β^-)-decay, one of the neutrons of the nucleus turns into a proton with the emission of an electron and an electron antineutrino $\tilde{\nu}_e$:

$$ {}^{A}_{Z}X_N \rightarrow {}^{A}_{Z+1}X_{N-1} + e^- + \tilde{\nu}_e, \quad \beta^- - decay. \tag{3} $$

Here A – the mass number, Z – the charge of a nucleus, N – the number of neutrons. In positron (β^+) decay, one of the protons of the nucleus turns into a neutron with the emission of a positron and an electron neutrino ν_e.

$$ {}^{A}_{Z}X_{N} \rightarrow {}^{A}_{Z-1}X_{N+1} + e^{+} + \tilde{\nu}_{e}, \quad \beta^{+-} - decay \quad . \tag{4} $$

Beta decay is closely related to the so-called reverse β-processes: capture of an electron from the K-shell of an atom (K-capture) or less likely to be captured from L- and other shells (electronic capture):

$$ e^{-} + {}^{A}_{Z}X_{N} \rightarrow {}^{A}_{Z-1}X_{N+1} + \nu_{e}, \tag{5} $$

and also reverse β-decay:

$$ \nu_{e}\,(\tilde{\nu}_{e}) + {}^{A}_{Z}X_{N} \rightarrow {}^{A}_{Z\pm1}X_{N\mp1} + e^{-}\,(e^{+}). \tag{6} $$

These processes are associated with neutrino processes:

$$ \tilde{\nu}_{e} + {}^{A}_{Z}X_{N} \rightarrow {}^{A}_{Z-1}X_{N+1} + e^{+}, \tag{7a} $$

$$ \nu_{e} + {}^{A}_{Z}X_{N} \rightarrow {}^{A}_{Z+1}X_{N-1} + e^{-}. \tag{7b} $$

If we do not take into account the structure of the nucleus, then at the level of nucleons the processes described above represent the following fundamental transitions (at the quark level):

$$ n \rightarrow p + e^{-} + \tilde{\nu}_{e}, \tag{8a} $$

$$ p \rightarrow n + e^{+} + \nu_{e}, \tag{8b} $$

$$ e^{-} + p \rightarrow n + \nu_{e}. \tag{8c} $$

β-decay of nuclei is possible in the case when the difference between the masses of the initial N and final N'-nuclei converts the sum of the electron masses m_e and neutrinos m_ν.

Energy conditions for β^--, β^+-decays and electron capture differ. When discussing the energy balance of these processes, we denote by $m(Z,A)$ the mass of a neutral atom (not a nucleus). We will not take into account the neutrino rest mass due to its smallness.

β^--decay. The β^--decay energy Q_{β^-} has the form

$$Q_{\beta^-} = \left[m(Z,A) - Zm_e\right]c^2 - \left[\left(m(Z+1,A) - (Z+1)m_e + m_e\right]c^2 = \right.$$

$$= \left[m(Z,A) - m(Z+1,A)\right]c^2 . \tag{9}$$

This so-called quantity Q_{β^-} in β^--decay corresponds to the difference in the masses of the parent and daughter atoms.

β^+-decay. Similarly for β^+-decay fair

$$Q_{\beta^+} = \left[m(Z,A) - Zm_e\right]c^2 - \left[\left(m(Z-1,A) - (Z-1)m_e + m_e\right]c^2 = \right.$$

$$= \left[m(Z,A) - m(Z-1,A)\right]c^2 . \tag{10}$$

Since the atomic masses are used, the energy at rest of the electron and positron is also taken into account.

Electronic capture (EC). With electronic capture, it turns out

$$Q_{EC} = \left[m(Z,A) - Zm_e\right]c^2 + mc^2 - \left[m(Z-1,A) - (Z-1)m_e\right]c^2 =$$
$$= \left[m(Z,A) - m(Z-1,A)\right]c^2 . \tag{11}$$

For the β-transition to occur, the corresponding quantity Q must satisfy the condition

$$Q_i > 0, \quad i = \beta^-, \beta^+, EC. \tag{12}$$

It is seen that electron capture is energetically more preferable than β^+-decay:

$$Q_{\beta^+} = Q_{EC} - 2m_e c^2 . \tag{13}$$

Emission of an electron is possible only when the mass difference between the parent and daughter atoms is at least not less than $2m_ec^2$. Due to the fact that β^+-decay and electron capture lead to the formation of the same daughter nucleus, electron capture is always a competing process for β^+-decay. If the mass difference Q_{EC} is in the range from 0 to $2m_ec^2$, then only electron capture is possible. Of course, in many cases, as a result of the β-transition, instead of the ground state of the daughter nucleus, its excited state is formed. An excited nucleus usually passes into the ground state by the emission of γ-quanta or conversion electrons. If the excitation energy exceeds the binding energy of a neutron or the fission barrier, then β-delayed emission of a neutron (proton) or β-delayed nuclear fission can occur. These processes are very important for the physics of reactors (delayed neutrons), as well as the synthesis of heavy elements in the Universe, etc. (see, for example, [1-22]).

When β^+-decay is energetically possible, electron capture is also possible. In some cases, the so-called double beta decay can occur: $A\ (Z,N) \rightarrow A\ (Z \pm 2,\ N \mp 2)$ with the emission of two β-particles and a neutrino pair, or without the emission of neutrinos.

The energy released during β-decay is distributed between the electron, neutrino and the final nucleus, and the overwhelming part is accounted for by light particles.

Therefore, the spectrum of emitted β-particles is continuous and their kinetic energy takes values from 0 to a certain boundary energy E_0, determined by the relation (see, for example, [3,5]):

$$E_0 / c^2 = M\ (A,Z) - M(\ A,\ Z+1) - m_e - m_\nu\,, \qquad (14)$$

where M – are the masses of the initial and final nuclei.

The foundations of the theory of beta decay were created by E. Fermi in 1934. Fermi proceeded from the four-fermionic interaction of nucleons and leptons by analogy with the effective electron-nucleon interaction in electrodynamics. In this case, it is important that, in contrast to the electromagnetic interaction, which is long-range, the four-fermionic Fermi interaction was contact (local). The Hamiltonian of the Fermi nucleon-lepton interaction is written in the form (see, for example, [1,3]):

$$H_\beta = G_\beta\,(\overline{\psi}_p \gamma_\mu\ \psi_n)\,(\overline{\psi}_e\ \gamma^\mu\ \psi_\nu)\,. \qquad (15)$$

Here G_β – is the coupling constant (Fermi constant); Ψ – four-component wave functions of interacting particles, satisfying the Dirac equation; $\overline{\psi}_e = \Psi + \gamma_0$ – conjugate wave functions; γ^μ – Dirac matrices, μ=0,1,2,3,4; $\gamma^0=\gamma_0$; $\gamma^i=-\gamma_i$ (i=1,2,3).

In the original version of Fermi's theory, the nucleon-lepton interaction had a purely vector form. Later it became clear that the weak interaction Hamiltonian can be a combination of relativistically invariant terms formed from a scalar (S), a pseudoscalar (P), a vector (V), an axial vector (A), and a tensor (T).

The discovery of spatial parity nonconservation, the study of the correlations between the directions of emission of β-particles and neutrinos in β-decay of ^{35}Ar and ^{6}He nuclei, as well as the angular distributions of electrons and neutrinos in the decay of polarized neutrons showed that β-decay is mainly realized in the V-A-variant. The effective β-decay Hamiltonian used in modern calculations was proposed by R.F. Feynman and M. Gell-Man in 1958 and is written in the following form:

$$H_\beta = \frac{G_\beta}{\sqrt{2}} J^\mu(x) L_\mu(x) + \text{h.c.} \qquad (16)$$

Here h.c. – these are Hermitian conjugate terms; J^μ – nucleon current; L_μ – lepton current; x – space-time coordinate; $G_\beta = G_\mu \cdot \cos\vartheta_c$, where G_μ – universal constant of weak interaction; multiplier $\cos\vartheta_c$ responds to processes without changing weirdness (ϑ_c – so called Cabibbo angle); Constant G_β =1,40 $\cdot 10^{-49}$ erg.cm^3 was found experimentally.

The lepton current L_μ is a combination of V–A terms with equal weights and is expressed through the wave functions of the electron and neutrin:

$$L_\mu(x) = \overline{\psi}_e(x)\,\gamma^\mu(1+\gamma_5)\,\psi_\nu, \qquad (17)$$

where $\gamma_5 = i\,\gamma_0\,\gamma_1\,\gamma_2\,\gamma_3$. The nucleon current J^μ is also a combination of the vector and axial-vector terms

$$J^\mu = V^\mu(x) - A^\mu(x). \qquad (18)$$

It cannot be written out explicitly in terms of the wave functions of nucleons; however, the matrix elements of V^μ and A^μ between the nucleon states, which de-

termine the characteristics of the nucleon-resonance, can be expressed through a small number of coupling constants g_V, g_M, g_S, g_p, g_T (see, for example, [1-5]):

$$<N'|\ V^{\pm}(0)\pm\ |N> = \bar{U}_{N'}[\ g_V(q^2)\ \gamma_\mu + \frac{g_M(q^2)}{2Mc}\sigma_{\mu\nu}q^\nu + g_S(q^2)q_\mu\ ]\tau^{\pm}U_N\ , \quad (19a)$$

$$<N'|\ A_\mu{}^{\pm}(0)\pm\ |N> = \bar{U}_{N'}[\ g_A(q^2)\ \gamma_\mu + g_P(q^2)q_\mu + \frac{g_T(q^2)}{2Mc}\ \sigma_{\mu\nu}q^\nu]\gamma_5\tau^{\pm}U_N\ , \quad (19b)$$

where N, N' – initial and final nucleons; U – Dirac bispinor (solution of the free Dirac equation); $\tau^{\pm}$ – increasing and decreasing isospin operators, converting neutron to proton and proton to neutron; $\sigma_{\nu\mu} = 1/2\ (\gamma_{\mu'}\gamma_\nu - \gamma_\nu\gamma_\mu)$; $N = 0,1,2,3$; $q_\mu = (P_{N'} - P_N)\mu$ – transmitted fourth pulse; $P_{N'}$ и P_N – momenta of the initial and final states of the nucleon. From the hypothesis of conservation of the vector current it follows that: $g_V \equiv g_V(0) = 1$, $g_S(q^2) = 0$, $g_M(0) = \mu_p - \mu_n = 3{,}70$, where μ_p, μ_n – abnormal magnetic moments of the proton and neutron in units nuclear magneton. Experimental studies of β-decay of nuclei have confirmed the hypothesis of conservation of the vector current and obtain a limitation on the constant g_T, which characterizes the axial current of the second kind: $|g_T/g_A| \le 10^{-4}$.

The energies released during β-decay are small compared to $m_N c^2$ (m_N – nucleon mass), therefore, it is natural to consider the transmitted fourth pulse q_M equal to 0. Then the one-nucleon Hamiltonian H_β is written in the form:

$$H_\beta = \frac{G_\beta}{\sqrt{2}}\{g_V(1L_0 - \alpha L) - g_A(\gamma_5 L_0 - \sigma L_0\}\tau^{\pm}. \quad (20)$$

Here g_V and g_A – vector and axial constants of nucleon-lepton interaction; 1 – single operator; $\alpha = \gamma_0\gamma$ – Dirac matrices; $\sigma = -\gamma_0\gamma\gamma_5$ – Pauli spin matrices. As a result, the effective β-decay Hamiltonian is determined by two coupling constants – the vector g_V and the axial-vector g_A.

Further development of the theory led to the creation of a unified theory of weak and electromagnetic interactions (and then the Standard Model), however, the existence of intermediate bosons has practically no effect on the theory of beta decay due to the smallness of the energy $E \le 10$ MeV in comparison with $m_W c^2$. For this reason, in fact, the theory of electroweak interactions for β-decay is reduced to the theory of Feynman and Gell-Mann (see explanation and citation Refs. in [1-4]).

1.2 Main characteristics of β-decay. Classification of β-transitions. Selection rules

As is known, the main characteristics of β-decay include the half-life $T_{1/2}$, the shape of β-spectra, $\beta^{\pm}$ - γ-angle correlations, etc. An analysis of the $fT_{1/2}$ values, together with the selection rules (see below), makes it possible to determine the unknown values of nuclear spins and parities, i.e. is one of the important methods of nuclear spectroscopy (see, for example, [3]). Since the $fT_{1/2}$ values are directly related to the matrix elements of β-transitions, they also contain information about the nuclear structure.

To determine the characteristics of beta decay, it is initially necessary to determine the amplitude of the process, which is determined by the matrix element of the transition between the initial i and final f nuclear states:

$$M_{fi} = \langle f \mid H_{\beta} \mid i \rangle. \tag{21}$$

In the case of β-decay of a nucleon, the desired matrix element:

$$M_{fi} = \int \psi_f^{+} (r_1, \ldots r_A) H_{\beta} (r_1, \ldots, r_A) \Psi_i (r_1, \ldots, r_A) d^3 r_1, \ldots, d^3 r_A, \tag{22}$$

where the effective Hamiltonian of the process H_{β} is equal to the sum of the terms describing the β-decay of individual nucleons that make up the nucleus:

$$H_{\beta} (r_1, \ldots, r_A) = \sum_{i=1}^{i=A} H_{\beta}^{i} (r_i), \tag{23}$$

where r – spatial coordinate of nucleons in the nucleus.

It should be emphasized here that the theory describes not only one-nucleon transitions. In the wave functions of the initial and final states of nuclei, it is possible to take into account the effects of a multi-nucleon structure, including the possibility of collective excitations of the nucleus [2-20]. Naturally, in this approximation, the so-called meband exchange currents, which describe the emission of the $e\tilde{\nu}_e$ $(e^{+} \nu_e)$ pair by virtual mesons, which are exchanged by nucleons in the nucleus, are not taken into account. Also, the emission of a lepton pair by nucleons, which occurs due to the exchange of virtual mesons, is not taken into account.

In fact, taking into account the meson exchange currents lead to the many-body operator H_{β}. It should also be added that the contributions of the sought-for

meson exchange currents to the β-spectra and half-lives can reach several percent. The β-particle spectrum is related to the matrix element M_{fi} by the following expression [4]:

$$N(E)\,dE = \frac{G_\beta^2}{2\pi^2 c^5 \hbar^7}\,|M_{fi}|^2 pE\,(E_0 - E)^2\,dE, \qquad (24)$$

where p and E – momentum and energy of the emitted β-particle;

In deriving expression (24), it was assumed that $m_\nu = 0$ and the recoil energy of the final nucleus is negligible compared to E_0. If M_{fi} does not depend on energy, then the shape of the β-spectrum is determined only by the "statistical" factor:

$$N(E) \sim pE\,(E_0 - E)^2. \qquad (25)$$

When calculating the matrix elements M_{fi}, a number of approximations are usually used, namely [3]: 1) the boundary energies E_0 are relatively small; therefore, the de Broglie wavelengths of the emitted leptons are large compared to the size R of the nuclei: $pR\,|\hbar << 1$, $qR\,|\hbar << 1$, those the wave functions of leptons vary slightly inside the nucleus; 2) being taken between nuclear states, some operators entering the formula for H_β have matrix elements of the order 1, whereas others have matrix elements of order v_N/c, where v_N – characteristic velocity of a nucleon in a nucleus.

For light and medium nuclei, the parameter $Ze^2\,|\,\hbar c << 1$. When calculating M_{fi}, an expansion in these small parameters is usually used. The neutrino wave function Ψ_ν entering the lepton part of the matrix element $L\mu(r)$ is described by a plane wave, i.e.:

$$\Psi_\nu(r) \sim \exp(-iqr\,|\,\hbar) \approx 1 - iqr\,|\,\hbar - 1/2(qr\,|\,\hbar)^2 + \ldots . \qquad (26)$$

Since it is obvious $qR\,|\,\hbar << 1$, then inside the nucleus $(r < R)$ $\Psi_\nu(r) \approx$ const, and upon integration over the volume of the nucleus, the neutrino wave function does not lead to the dependence M_{fi} from E. In the approximation of neglecting the interaction of the emitted β-particle with the Coulomb fields of the nucleus and the electron shell of the atom, its wave function can also be represented as a plane wave, i.e.:

$$\Psi_e(r) = \exp(-ipr\,|\,\hbar). \qquad (27)$$

Taking into account the Coulomb fields of the nucleus and the electron shell of the atom leads to a difference between the wave function and a plane wave; as a result, the wave function becomes dependent on the energy E even at $pr|\hbar << 1$. Note that initially this circumstance was ignored and this often predetermined a significant error in calculating the characteristics of beta decay [4]. To take into account the influence of the Coulomb interaction of the emitted β-particles on their energy spectrum, the so-called Coulomb correction factor is introduced, which is determined by the known Fermi function $F(Z,E)$. When $pr|\hbar << 1$ this factor is usually defined as the square of the ratio of the β-particle wave functions calculated with ($Z \neq 0$) and without ($Z = 0$) the Coulomb field of the nucleus at the center ($r = 0$) or at the periphery ($r = R$) of the nucleus, i.e. [4,12,13]:

$$F(Z,E) = |\Psi_e|^2_z / |\Psi_e|^2_0. \qquad (28)$$

The approximation, in which only the leading nucleon contributions to the Hamiltonian H_β are taken into account, and the lepton wave functions inside the nucleus are assumed to be independent of coordinates, is called allowed in the theory of beta decay. In this approximation, the spectrum of β-particles is described by the expression:

$$N(E)\,dE = \frac{m_e^5 c^4}{2\pi^3 \hbar^7} G_\beta F(Z,E \left\{ n^2 V |\int 1|^2 + g^2 A |\int \sigma|^2 \right\} \times$$

$$\text{x}\; E\sqrt{E^2 - 1}\; (E_0 - E)^2 dE. \qquad (29)$$

Here the energy is expressed in units of $m_e c^2$ (m_e – is the electron mass);

$$\int 1 \equiv \left\langle f \mid \sum_{i=1}^{A} \tau_\pm^{(i)} \mid i \right\rangle ,$$
$$\int \sigma \equiv \left\langle f \mid \sum_{i=1}^{A} \sigma^{(i)} \tau_\pm^{(i)} \mid i \right\rangle . \qquad (30)$$

The first relation corresponds to the vector interaction C_V and is called the Fermi matrix element, and the second relation corresponds to the axial-vector interaction C_A and is called the Gamow-Teller matrix element. In the general case, it is

not possible to determine $| i >$, $< f |$ which correspond to the initial and final states of the nucleus.

However, if we take the spin I and parity π of the states of the nucleus, between which the β-transition is observed, as a basis for consideration, then we can derive selection rules (see below) for the nuclear matrix elements that arise in the series expansion of the interaction Hamiltonian and, in particular, the above nuclear matrix elements. Functions $| i >$ and $< f |$ can be formally represented:

$$| i >=< \tilde{i} I_i (M_i) >, \tag{31a}$$

$$< f | =< I_f (M_f) \tilde{f} >, \tag{31b}$$

where I_i, I_f – the initial and final spins of the states of the mother and daughter nuclei, between which there is β-transition; M_i, M_f – their projections respectively; $\tilde{i}$, $\tilde{f}$ – quantities that include all the remaining characteristics of the nuclei. This approach allows us to rewrite the expression for nuclear matrix elements in the form:

$$\int 1 = \left\langle I_f (M_f) \tilde{f} \left| \sum_{s=1}^{A} \tau_{\pm}^{s} \right| \tilde{i} I_i (M_i) \right\rangle \tag{32a}$$

$$\int \boldsymbol{\sigma} = \left\langle I_f (M_f) \tilde{f} \left| \sum_{s=1}^{A} \boldsymbol{\sigma}^{s} \tau_{\pm}^{s} \right| \tilde{i} I_i (M_i) \right\rangle \tag{32b}$$

To obtain selection rules for the total angular momentum of a lepton pair J, it is necessary to use the Wigner-Eckart theorem, which allows one to separate the parts associated with the spin projections from the corresponding nuclear matrix elements and proceed to the consideration of the reduced matrix elements (see below).

Further, it is important to note that it is obvious that the Coulomb field of the nucleus increases the probability of the emission of electrons and decreases the probability of the emission of positrons in the low-energy region. In addition, when the Fermi factor $F(Z, E)$ is taken into account, the probability of electron emission during beta decay at the lower boundary of the β-spectrum does not vanish, but tends to a finite value. The influence of the Coulomb factor on the β-

spectra and the probability of beta decay increase with increasing Z and decreasing E_0. When calculating F (Z, E), it is also necessary to take into account the screening of the nuclear charge by atomic electrons (it is especially important in the case of β^+-decay).

It should be emphasized here that this effect has not yet found an adequate quantitative description in modern calculations (e.g. [1-13]. In many papers (e.g. [1-30] the possibility of influencing the processes of nuclear decay with the participation of electrons of the atomic shell (*K*-capture and internal conversion) by ionizing the atom was considered. In the German research center GSI, it was experimentally shown that the effect of the presence or absence of electron shells in an atom can significantly change the entire decay scheme and, accordingly, the quantitative characteristics (e.g. [3]).

The total probability W of beta decay per unit time can be obtained by integrating (29) over energy and has the form:

$$W = \frac{m_e^5 c^4}{2\pi^3 \hbar^7} G_\beta \left\{ g^2 V |\int 1|^2 + g^2 A |\int \sigma|^2 \right\} f , \qquad (33a)$$

$$f = \int_1^{E_0} F(Z,E)\ E\sqrt{E^2-1}\ (E_0 - E)^2 dE. \qquad (33b)$$

In the case of neglecting the interaction of the emitted β-particle with the Coulomb field of the atom, one can obtain:

$$f|_{Z=0} = \int_1^{E_0} E\sqrt{E^2-1}\ (E_0 - E)^2 dE =$$

$$= \sqrt{E^2-1}\left[\frac{E_0^4}{30} - \frac{3E_0^2}{20} - \frac{2}{15}\right] + \frac{E_0}{4}\ln\left(E_0 + \sqrt{E_0^2-1}\right). \qquad (34)$$

The f value is calculated using the tabulated values of the Fermi function $F(Z, E)$ [3,12]. In the general case, $F(Z,E)$ is defined as the ratio of the probabilities of finding an electron at a certain point with Z = 0 and without Z ≠ 0 taking into account the field of the atom:

$$F(E,Z) = |\psi|^2_{Z\neq 0} \Big/ |\psi|^2_{Z=0} . \qquad (35)$$

A remarkable feature of the allowed transitions is the fact that all nuclear β-moments are concentrated in one factor, and the energy dependence is due only to a statistical factor and a function $F(Z,E)$.

Thus, in the expression for the normalized β- and $\tilde{\nu}$-spectra, the factor

$$\left[C_V^2 <\mathbf{1}>^2 + C_A^2 <\boldsymbol{\sigma}>^2 \right]$$

can be taken out from under the integral sign, and after abbreviations, the final expressions for calculating the spectra of allowed transitions can be obtained. By definition, the half-life $T_{1/2}$ is related to the beta-decay probability W by the standard ratio:

$$W = ln2 / T_{1/2}. \qquad (36)$$

Then you can write:

$$f T_{1/2} = k / \left\{ g^2 V \mid \int 1 \mid^2 + g^2 A \mid \int \sigma \mid^2 \right\}, \qquad (37)$$

where $k = 2\pi^3 ln\, 2 \hbar^7 / m_e^5 c^4 G_\beta^2 = G_\beta^{-2} \cdot 12306$ s. The $fT_{1/2}$ value is usually called the comparative half-decay period and plays an important role in the classification of β-transitions (see below). The function f takes into account the dependence of the beta decay probability on E_0 and Coulomb effects; therefore, $fT_{1/2}$, in contrast to the standard half-life $T_{1/2}$, depends only on M_{fi}.

Next, we briefly consider the main classification of β-transitions. It should be noted right away that beta decay is characterized by a wide range of changes in the half-lives of $T_{1/2}$, usually from 10^{-2} s to 10^{16} years. Such a significant variation in the $T_{1/2}$ values is explained by several reasons. First of all, this is due to the fact that the half-life strongly depends on E_0 (at $E_0 >> m_e c^2$, $W \sim E_0^5$), and the value of E_0 varies widely from 2,64 keV for the $^{187}Re \rightarrow ^{187}Os$ transition to 13,43 MeV for $^{12}B \rightarrow ^{12}C$. On the other hand, depending on the spins and parities of the initial and final nuclear states, various terms in the effective beta decay Hamiltonian, whose matrix elements have different orders of magnitude, contribute to the process amplitude. Finally, the lepton pair emitted during beta decay can carry away different orbital angular momentum.

With an increase in this moment, due to the centrifugal effect, the values of the wave functions of leptons in the intranuclear region, and, consequently,

the overlap integral of wave functions, which determines the matrix element M_{fi} Accordingly, all β-transitions are divided into allowed and forbidden.

Let's consider the allowed transitions first. In the allowed approximation, the wave functions of leptons inside the nucleus are constant, and leptons do not carry away the orbital angular momentum.

Moreover, if the spin of the nucleus does not change, then the total spin carried away by the lepton pair is also equal to 0. Such transitions are called Fermi transitions.

In the case when the vector change in the nuclear spin (the total spin carried away by the lepton pair) is equal to 1, then, by definition, these transitions are called Gamow-Teller. The parity of nuclear states in allowed β-transitions does not change. As a result of the selection, the rules limiting the change in the total moment I and the parity π of the nucleus, in the case of allowed transitions of the Fermi type, are written in the form: $\Delta I = | I_f - I_i | = 0$; $\Delta\pi \equiv \pi_f \pi_i = +1$. For Gamow-Teller transitions, similar selection rules are: $\Delta I = 1$, $\Delta\pi = +1$.

Table 1 – Characteristics of some super-allowed β-transitions

Transition	$I_i^{\pi_i} \rightarrow I_f^{\pi_f}$	$T_{1/2}$		E_0, keV	$fT'_{1/2}$
n→ p	½$^+$→½$^+$	11,7+0,3 min		782±1	1187±35
^{3}H→^{3}He	½$^+$→½$^+$	3,87· 10^8 s		18,65±0,	1132±40
^{6}He→^{6}Li	0$^+$→1$^+$	0,813±0,7 s		3500±2,0	808±32
^{17}F→^{17}O	5/2$^+$→5/2$^+$	66,0±0,5 s		1748±6	2380±40
^{35}Cl→^{35}Ar	3/2$^+$→3/2$^+$	1,804±0,21 s		4948±30	5680±400
^{14}O→^{14}N	0$^+$→0$^+$	71,36±0,09 c		1012,6±1,4	3066±10
^{34}Cl→^{34}S	0$^+$→0$^+$	1,565±0,07 s		4460±4,5	3055±20
^{42}Sc→^{42}Ca	0$^+$→0$^+$	0,6830± 0,0015		5409±2,3	3077±9
^{46}V→^{46}Ti	0$^+$→0$^+$	s		6032,1±2,2	3088±8
^{50}Mn→^{50}Cr	0$^+$→0$^+$	0,4259±0,0008 s		6609,0±2,6	3082±9
		0,2857±0,0006 s			

Further, in the modern classification, allowed transitions are subdivided into super-allowed and hindered. The first include transitions between nuclear states with similar wave functions, as a result of which the integrals of their overlap are large ($\int \sim 1$, $\int\sigma \sim 1$), and the values $fT_{1/2}$ take minimum values. The super-allowed transitions include, in particular, transitions between states belonging to the same isomultiplet (between analog states of nuclei). For supersolved $\beta^{\pm}$-

transitions, $\int 1$ can be calculated exactly [2-4]. The fact is that $\sum_{i=1}^{A} \tau_{\pm}^{i} = T_{\pm}$, where T is the isotopic spin of the initial nucleus. Wherein: $\int 1 = [(T \mp T_3) \cdot (T \pm T_3 + 1)]^{1/2}$. Here T_3 is the isospin projection for the initial nucleus, numerically equal to ½ (Z - N) (it is assumed that the β-transition occurs between pure isospin states; taking into account the meson exchange currents does not change this result, which is due to the conservation of isospin).

In the case of super-allowed transitions $0^+ \rightarrow 0^+$ between neighboring terms of the isomultiplet: $\int \sigma = 0$ and, at T = 1: $\int 1 = \sqrt{2}$.

For such super-resolved transitions, the $f\ T_{1/2}$ values should be the same, which is in good agreement with available data (see Table 1) [2,3]. Relation (37) allows you to determine the value of G_β from the measured values of $f\ T_{1/2}$ for $0^+ \rightarrow 0^+$ transitions:

$$G_\beta = (1{,}4057 \pm 0{,}0016 \pm 0{,}0070) \cdot 10^{-49} \text{ erg. cm}^3. \qquad (38)$$

Further, we note that the Gamow-Teller transitions $0^+ \rightarrow 1^+$ are characterized by a single matrix element $\int \sigma \neq 0$ and can be used to obtain information on the value of the axial-vector coupling constant g_A. The most accurate value g_A= -1,254±0,007 was obtained from the data on β-decay of the neutron.

The so-called hindered transitions differ from the super-allowed transitions by a relatively weak overlap of the wave functions of the initial and final nuclear states, as a result of which the matrix elements turn out to be small compared to the matrix elements of the super-allowed transitions [2-4]. An example of hindered transitions is the $0^+ \rightarrow 0^+$ transitions between states belonging to different isospin multiplets. Such transitions satisfy the Fermi-type selection rules ΔI=0, $\Delta \pi$=+1б, and are described by a single matrix element $\int 1$. If the initial and final nuclear states are pure isospin states belonging to different isomultiplets, $\int 1$=0 and the transition probability W=0.

It should be remembered that the Coulomb interaction in nuclei violates isotopic invariance. Then the nuclear states (especially in heavy nuclei) are not pure and contain impurities of states with a different isospin. As a result, the matrix elements of such transitions are not equal to 0. They are small compared to the usual allowed matrix elements, although the spin and parity selection rules are satisfied.

Another type of β-transitions is called forbidden transitions. Selection rules for matrix elements of forbidden transitions are derived similarly to the case of allowed transitions, while the expression for the matrix element after applying

the procedure for separating the reduced matrix elements (β-moments) has a rather complicated and inconvenient form for practical use. To simplify it, the so-called normal approximation is used, based on the fact that nuclear β-moments have different orders of magnitude. The small parameters by which these quantities are estimated are: nucleon velocity V_N, nucleus radius R, Coulomb smallness parameter aZ.

The order of smallness of the β-moments included in the expansion of the matrix element determines the degree of inhibition of β-transitions.

Forbidden transitions include transitions in which a lepton pair carries away the orbital angular momentum and (or) the main contribution to the process amplitude is made by small matrix elements from the operators γ_5,α in the effective Hamiltonian H_β. Forbidden transitions are classified according to the degree of smallness of the matrix element. Transitions of the first order of exclusion include transitions described by matrix elements $\int\alpha$, $\int r$, $\int\gamma_5$, $\int[\sigma r]$, $\int(\sigma r)$, $\int B_{ij}$, where

$$\int\alpha=\langle f \mid \sum_{a=1}^{A} \alpha^a \tau_\pm^a \mid i\rangle; \int r =\langle f \mid \sum_{a=1}^{A} r^a \tau_\pm^a \mid i \rangle \text{ etc.},$$

$$B_{ij}\equiv\sigma_i x_j+\sigma_j x_i 2/3(\sigma r)\sigma_{ij};\ i, j = 1,2,3;$$

x_i – vector component r.

The first 2 matrix elements are due to the vector current, the rest - to the axial one. Matrix elements containing the value r arise when a lepton pair carries away the orbital angular momentum 1. Selection rules for matrix elements $\int\gamma_5$, $\int(\sigma r)$ are as follows: $\Delta I = 0$, $\Delta\pi = -1$. For $\int\alpha$, $\int r$ and $\int[\sigma r]$, the selection rules are: $\Delta I^{\Delta\pi} = 1^-, 0^-$ (transitions $0\leftrightarrow 0$ are prohibited).

In the transitions described by matrix transitions of the first forbidden, the lepton pair carries away the total moment 2, and the selection rules are as follows: $\Delta I^{\Delta\pi} = 2^-, 1^-, 0^-$ (forbidden transitions $0\leftrightarrow 0$, $0\leftrightarrow 1$, $1/2\leftrightarrow ½$). The matrix elements $\int\gamma_5$ and $\int\alpha$ are of order of smallness (v_N/c). For matrix elements containing r, it is natural to expect that the order $pR|\hbar \le E_0R|\hbar c$. However, this is only true for unique transitions. For the rest of the matrix elements, in the case when the nuclear charge Z satisfies the so-called ξ-approximation $\xi \equiv (Ze^2/rE_0) >> 1$) [4], Coulomb effects lead to an increase in the wave function of the electron inside the nucleus. As a result, these matrix elements are of the order of smallness $Z/137$ rather than $pR|\hbar$. Note that the condition $\xi >>1$ holds for most β-transitions. With an increase in the order of exclusion, the number of the corresponding matrix elements that determine the transition probability

increases, and the difficulty of analyzing the experimental data increases; in this case, the matrix elements themselves decrease in order of magnitude [4]. Selection rules for β-transitions of the nth order of prohibition: $\Delta\pi = (-1)^n$, $\Delta I \leq n$ for ordinary transitions and $\leq n+1$ for unique transitions. With an increase in n and a decrease in matrix elements, the value of $fT_{1/2}$ increases.

Although the range of its variation is narrower than for $T_{1/2}$, it turns out to be quite large, so here it is convenient to characterize β-transitions by the value $lg\, f\, T_{1/2}$ (see Table 2).

Table 2 – Selection rules for β-transitions of various types

Transition type	Selection rules	$lg\, fT_{1/2}$	$lg\, fnT_{1/2}$
Allowed over-	ΔI =0,1	3,5±0,2	
authorized	$\Delta\pi$=+1	5,7±1,1	
hindered			
	ΔI =1,0	7,5±1,5	
Forbidden	$\Delta\pi$=-1		
first ban ….	ΔI =2		8,5±0,7
	$\Delta\pi$=-1		
uniquefirst ban ….			
	ΔI =2		
second ban	$\Delta\pi$=+1	12,1±1,0	
	ΔI =3		11,7±0,9
unique second	$\Delta\pi$=+1		
prohibition ….			
	ΔI =3	18,2±0,6	
third ban	$\Delta\pi$=-1		
	ΔI =4		15,2(^{40}K)
unique third prohi-	$\Delta\pi$=-1	22,7(^{115}ln)	
bition ….	ΔI =4		
fourth ban	$\Delta\pi$=+1		

Further, before proceeding to a detailed analysis of the current state of calculations of the characteristics of beta decay, we note some experimental aspects of the problem, following [2,4]. Usually β-spectra are experimentally investigated, as a rule, using beta-spectrometry. In the case of allowed transitions, the β-spectra are described by the expression:

$$N(E)dE \sim F(Z,E)pE(E_0 - E)^2 dE. \quad (39)$$

To study β-spectra, so-called Curie plots are usually used, which depict the dependence of the quantity $K \equiv [N(E)F(Z,E)pE]^{1/2}$ from E.

For allowed transitions, the Curie graph has the form of a straight line segment intersecting the abscissa axis at the point $E=E_0$. More precisely, the shape of the observed spectrum is:

$$N(E_e) = \frac{V^2}{2\pi^3 c^5 \hbar^7} \overline{\left|\langle f|H_\beta|i\rangle\right|^2} E_e p_e (E_0 - T_e)^2 . \quad (40)$$

This expression qualitatively explains the shape of the observed β-spectrum and is usually used for the experimental determination of the boundary β-decay energy. After dividing the left side of (40) by $E_e p_e$, and then extracting the square root of this value, you can get a function that is linearly dependent on the kinetic energy of the electron T_e. The graph of this function, the Curie graph is described by the equation:

$$\left(\frac{N(E_e)}{E_e p_e}\right)^{1/2} = const \cdot \overline{\left|\langle f|H_\beta|i\rangle\right|^2} (E_0 - T_e). \quad (41)$$

The graph is a straight line only if the matrix element really does not depend on the electron momentum, which occurs in the case of allowed β-transitions. It is very convenient to find the boundary β-decay energy E_0 from the graph, since the function should vanish exactly at E_0. The deviations from the linear dependence can be used to study with very good accuracy the influence of corrections due to the nonzero neutrino mass.

So far, the spectrum has been calculated under the assumption that $m_\nu=0$. With a finite neutrino rest mass, one should expect a change in the shape of the spectrum in the region of maximum values of the energy variable, since the neutrino mass is small ($m_\nu << m_e$). In particular, the end point of the β-spectrum E_{max}, equal to the maximum possible kinetic energy of an electron, will be shifted by the amount of the neutrino rest energy $E_{\max} = E_0 - m_\nu c^2$.

Differences in the transition from the allowed one leads to violation of the linearity of the Curie graph. The beta spectra of forbidden transitions can differ

significantly from the allowed spectra due to the presence of energy-dependent terms in the matrix element. This effect is usually taken into account by introducing an energy-dependent spectral form factor $S(E)$ into the right-hand side of expression (39). For unique first-forbidden transitions (neglecting Coulomb effects), this factor has the form: $S \sim [(E^2 - m_e c)^2 + (E_0 - E)^2]$.

Unique transitions of the nth prohibition are usually not characterized by the values $fT_{1/2}$, but $f_nT_{1/2}$, where f_n is determined by a formula of the form (33b), and then the form factor $S_n(E)$ is introduced into the integrand (see also Table 2). The energy spectra of ordinary (not unique) first-forbidden transitions are, as a rule, close to the allowed ones. Matrix elements $\int\gamma_5$ and $\int\alpha$ practically do not contain dependence on the lepton energy; for matrix elements $\int r$, $\int(\sigma r)$ and $\int[\sigma r]$, in the case $\xi >> 1$ the spectral form factor does not depend on energy due to Coulomb effects. An exception is some β-transitions of the 1st forbidden, in which the main energy-independent terms in the matrix element cancel each other out and small corrections depending on the energy begin to play a significant role. This situation is realized, for example, in the case of the β-decay of ^{210}Bi (Ra E) [2,4].

In many cases, beta decay occurs not into one state of the daughter nucleus, but into two or more states.

In this case, the experimentally observed β-spectrum is composed of two or more partial spectra with different values of the boundary energies. Such β-spectra are usually called complex.

Investigation of β-spectra near E_0 allows obtaining information on the neutrino mass mν. In the case $m_\nu \neq 0$, the spectrum of allowed transitions should differ from (39) and should have the form:

$$N(E)dE \sim F(ZE)pE(E_0 - E)[(E_0 - E)^2 - (m_\nu c^2)^2]^{1/2}. \qquad (42)$$

Hence it follows that the shape of the spectrum near E_0 depends substantially on m_ν.

The difference between m_ν and 0 can lead to a deviation of the Curie plot in the region E_0 from the linear one. In fact, to determine mν, it is necessary to compare the Curie plot with those calculated at different values of m_ν, depending on $K(E)$. β-spectrum studies ^3H (E_0 = 18661keV) gave $m_\nu < 35$ eV/s^2. Results obtained with emission of the β-spectrum ^3H: 14 eV< m_ν < 46 eV need further confirmation.

The current state of this problem has been described in Refs. [2,3].

1.3 Theoretical method. Relativistic Many-body Perturbation Theory

1.3.1 Determination of the probability of beta decay. Allowed and over-allowed transitions

As is known [4], the perturbation theory method is usually used in calculating the probability of β-decay, since the corresponding interaction constant g is characterized by significant smallness. For this well-known reason, in practice, the calculations are limited to taking into account only first-order terms corresponding to direct transitions from the initial state to the final state. The probability of a system transition from an initial state $|\xi>$ with energy E_ξ to a certain final state $< f |$ with energy E_f per unit time under the condition $E_0 = E_f - E_\xi$ is determined by the well-known expression:

$$dW_{\xi f} = \frac{2\pi}{\hbar} |< f \mid H \mid \xi >|^2 \left. \frac{d\tilde{N}}{dE} \right|_{E=E_0}, \qquad (43)$$

where, naturally, the matrix element is determined by the form of the interaction Hamiltonian H_β and the wave functions of the initial ψ_ξ and final ψ_f states of the nucleus:

$$< f \mid H \mid \xi >= \int \psi_f H_\beta \psi_\xi d^3 r_1 \ldots d^3 r_A \,. \qquad (44)$$

The determination of the square of the matrix element is reduced to integration over the volume of the kernel and averaging over all unobservable variables.

The quantity $\left. \frac{d\tilde{N}}{dE} \right|_{E=E_0}$ determines the density of the final states of the system per unit of energy. The expression for the number of β^-, $\tilde{\nu}$-particles with energies in the range from E to $E + dE$:

$$dW_{\xi f} = \frac{1}{2\pi^3 \hbar^7 c^5} |< f \mid H_\beta \mid \xi >|^2 \sqrt{E_e^2 - m^2 c^4}\, E_e \left(E_0 - E_e\right)^2 dE_e, \qquad (45a)$$

$$dW_{\xi f} = \frac{1}{2\pi^3\hbar^7 c^5}\left|< f \mid H_\beta \mid \xi >\right|^2 \sqrt{\left(E_0 - E_{\tilde{\nu}}\right)^2 - m^2c^4}\left(E_0 - E_{\tilde{\nu}}\right)E_{\tilde{\nu}}^2 dE_{\tilde{\nu}}. \quad (45b)$$

In what follows, we restrict ourselves to considering allowed and over-allowed transitions. It is generally known that allowed transitions make the most significant contribution to the total spectrum of β-decay of a nucleus, while the contribution of forbidden transitions usually amounts to only a few percent of the total intensity. The specific contribution of these and other transitions to the β-decay probability is usually described using in the expression for the Hamiltonian of the interaction and the β-decay probability of the expansion of the lepton current in a series in terms of small parameters characteristic of β-decay (see [2-3]). Where the zero term of such an expansion describes the most intense allowed β-transitions, and the next terms of the expansion correspond to forbidden transitions of various degrees of forbiddenness.

Let us consider further the allowed transitions in more detail. The energy distribution of β-particles in this case has a standard form:

$$dW_\beta(E)/dE = \frac{1}{2\pi^3} G_F^2 \cdot F(E,Z) \cdot E \cdot p \cdot (E_0 - E)^2 \cdot |M|^2 . \quad (46)$$

$$E_0 = 1 + (E_{гр}/m_e c^2),$$

Here G_F – is the weak interaction constant; E, $p=(E^2-1)^{1/2}$ – total energy and momentum of a β-particle; ($E_{гр}$ – β-spectrum boundary energy); $|M|$ – energy-independent matrix element for allowed β-transitions. F – the well-known Fermi function, which is equal by definition:

$$F(E,Z) = \frac{1}{2p^2}\left(g_{-1}^2 + f_{+1}^2\right), \quad (47)$$

where are the icons $\pm 1 = \kappa$, $\kappa = (l-j)/(2j+1)$.

In (47), functions f_{+1} and g_{-1}-relativistic electron radial wave functions appear, which are calculated at the boundary of a spherical nucleus with radius R_0 (see, for example, [2,4]) or the values of these functions at zero (amplitudes of the expansion of functions in a series at zero), as done in [3,12,13). In our calcu-

lations, we use the latter option everywhere. The corresponding integral Fermi function f is given by the definition:

$$f(E_0, Z) = \int_1^{E_0} F(E, Z) \cdot E \cdot p \cdot (E_0 - E)^2 dE. \qquad (48)$$

The half-life of beta decay in this notation is:

$$T_{1/2} = 2\pi^3 \ln 2 / [G^2 |M|^2 f(E_0, Z)]. \qquad (49)$$

An important point of the theory is the correct normalization of the relativistic electron radial functions f_κ and g_κ, at which, for large values of the radial variable

$$g_t(r) \rightarrow r^{-1} [(E+1)/E]^{1/2} \sin(pr + \delta_t), \qquad (50a)$$

$$f_t(r) \rightarrow r^{-1} (\iota/|\iota|) [(E-1)/E]^{1/2} \cos(pr + \delta_t). \qquad (50b)$$

A detailed description of the methodology for calculating the electronic and nucleon wave functions within the framework of the formalism of the relativistic nuclear and QED TV is given in reviews [21-46] (see also [47-61]). Here, we note that the numerical solution of all equations, as well as the entire calculation of the characteristics of β-decay and atomic corrections were performed on the basis of a modified numerical complex "Superatom-M". The functions of the continuous spectrum were found iteratively in the field of the daughter atom. The condition for the self-consistency of the functions of the continuous spectrum is reduced to the fact that the normalized functions at two adjacent iterations differ by less than 10^{-5} in relation to their values at the maximum point of the function. For different energies, to achieve the required accuracy, it was required from 3 (at higher energy) to 11 (at low energy) iterations.

When calculating the normalizing factor, the procedure of averaging over the oscillation period of the continuous spectrum function was used (the matching condition included the difference between the values of the averaged normalizing factors at two adjacent periods of no more than 0,025%).

To achieve the required accuracy, the Dirac equations were integrated (on a semilogarithmic scale) to the distances from the core, at which the continuum function passes 6-8 periods. As usual, when calculating the integrals of strongly

oscillating functions, the damping factor exp (-dr) was introduced, the value of the parameter d in which was chosen based on the accuracy requirement at a level of ~0,005%.

1.3.2 Combined Nuclear and Relativistic Many-body Perturbation Theory

Here we present a brief description of the key moments of our approach **(**more details can be found in refs. [21-60]). Fundamental spacts of accouting for the QED radiative corrections and physical nature of these ones is described in Refs. [61-85]. Within our approach, the electron wave functions zeroth basis is found from the generalized Dirac-Koihn-Sham equation solution with a mean-field self-consistent potential:

$$V_{MF} = V^{DKS}(r) = [V^{D}_{Coul}(r) + V_X(r) + V_C(r \mid b)] \tag{51}$$

Here $V^{D}_{Coul}(r)$ is the standard Coulomb-like potential, $V_C(r \mid b)$ is a correlation potential (the known Lundqvist-Gunnarsson-like definition for $V_C(r \mid b)$ with ab intio optimization parameter *b* is used; for details, see below and Refs. [10,48-52]) and $V_X(r)$ is an exchange potential [2].

The known Kohn-Sham definition for $V_X(r)$ is as follows (in atomic units):

$$V_X[\rho(r), r] = V^{KS}_X(r) \cdot \{\frac{3}{2} \ln \frac{[\beta + (\beta^2 + 1)^{1/2}]}{\beta(\beta^2 + 1)^{1/2}} - \frac{1}{2}\}, \tag{52}$$

where

$$\beta = [3\pi^2 \rho(r)]^{1/3} / c \ . \tag{53}$$

In order to describe a nuclear subsystem we use the known relativistic mean-field model [2,3]. In concrete calculation the most preferable version of this model is so called NL3-NLC version (c.g., Ref. [2,3,16,62]).

The total relativistic Dirac Hamiltonian for a multielectron system has the following form [2,10]:

$$H = \sum_i \{\alpha c p_i - \beta c^2 - Z / r_i\} + \sum_{i>j} \exp(i \mid \omega \mid r_{ij})(1 - \alpha_i \alpha_j)/r_{ij} \ , \qquad (54)$$

where α_i ,α_j are the Dirac matrices, ω_{ij} is the transition frequency. It should be noted that the magnetic interaction in the lowest order on parameter of the fine structure constant α^2 (α is the fine structure constant) as well as the retarding effect are taken into account in the relativistic interelectron interaction potential.

As it is indicated earlier, all correlation corrections of the second order and dominated classes of the higher orders diagrams are taken into account within a formalism of many-body perturbation theory [2,3,10].

The principal important piont of a total approach is in using a generalized relativistic energy approach to construction of an optimized basis set of electron wave functions. According to Glushkov-Ivanov-Ivanova method [48,49,52,53] optimization of electron wave function set and gauge invariance performance can be reached by means of the minimization of contribution into imaginary part of radiation width Im δE for the multi-electron system due to the QED perturbation theory fourth order Feynman diagrams ones. The detailes of a whole procedure can be found in Refs. [2,3,10,48,49,52,53].

The next very important aspect of a whole procedure is an accurate consideration of the QED or radiation corrections. There are developed a few accurate methods of accoutnig fior the QED corrections. In our approach we use the generalized procedures, described in detail in Refs. [2,10,50,63,67].

In order to account for a vacuum polarization effect, the generalized Uehling-Serber potential approach is used and modified to account for the high-order radiative corrections according to the procedure [2,10]. It can be represented in the following form:

$$U(r) = -\frac{2\alpha}{3\pi r} \int_1^\infty dt \exp(-2rt/\alpha Z)\left(1 + 1/2t^2\right)\frac{\sqrt{t^2-1}}{t^2} \equiv -\frac{2\alpha}{3\pi r} C(g), \qquad (55)$$

where $g=r/(\alpha Z)$.

A more correct and consistent approach is presented in Refs. [2,10]. Taking into account the nuclear finite size effect modifies the potential (55) as follows:

$$U^{FS}(r) = -\frac{2\alpha^2}{3\pi} \int d^3r' \int_1^\infty dt \exp\left(-2t|r-r'|/\alpha Z\right) \times \left(1 + \frac{1}{2t^2}\right)\frac{\sqrt{t^2-1}}{t^2}\frac{\rho(r')}{|r-r'|}, \qquad (56)$$

Other details of the general method and PC code are described in Refs. [2,10,21-45]. All calculations are performed with using the numeral codes SuperAtom (Nucleus) (modified versions 93) [21-61,85-108].

1.4 Results

Characterization of a number of allowed beta transitions and the results of calculating the characteristics of beta decay. The following beta decays were selected as objects of study, the results of which will be presented below (their characteristics are given in Table 3): $^{33}P \rightarrow ^{33}S$, $^{35}S \rightarrow ^{35}Cl$, $^{45}Ca \rightarrow ^{45}Sc$, $^{63}Ni \rightarrow ^{63}Cu$, $^{106}Ru \rightarrow ^{106}Rh$, $^{155}Eu \rightarrow ^{155}Gd$, $^{241}Pu \rightarrow ^{241}Am$.

Most of the considered beta decays belong to the number of transitions with a low boundary energy and correspond to different ranges of values of the atomic nucleus charge Z (see Table 1). Almost all transitions, the characteristics of which are given in Table 1, are allowed (as well as super-allowed). The choice of such transitions, naturally, is determined by the important circumstance that for such transitions the formulas for the decay probability are exact.

Of course, for forbidden beta transitions, the theory naturally becomes more complicated. The corresponding formulas are more complicated than in the case of allowed transitions and should generally contain six nuclear matrix elements. A detailed presentation of the theoretical aspects of their calculation is given, for example, in [2,4].

In the so-called ξ-approximation known in the theory of beta decay, where the parameter ξ is introduced, determined by the expression: $\xi = \alpha Z / 2R_0 >> 1$, (Z – the nuclear charge, R_0 – the radius) usually neglect small terms, and the remaining sum of nuclear matrix elements does not give an additional dependence on the lepton energy and turns out to be analogous to the allowed case. Moreover, it is written as a constant factor $|M|^2$.

Recall that if the condition ξ-approximation $\xi >> 1$ is satisfied, the Coulomb effects lead to an increase in the wave function of the electron inside the atomic nucleus, as a result of which these matrix elements are of the order of smallnes $\sim Z/137$, and no $pR|\hbar$. At the same time, it is well known that the sought condition $\xi >> 1$ turns out to be satisfied for most β-transitions.

Returning to the transition $^{241}Pu \rightarrow ^{241}Am$, it should be noted that this transition is not a unique one of the first ban. The parameter ξ for the decay of pluto-

nium is $\xi = 18$ (i.e. $\xi >> 1$). It is well known that for the overwhelming majority of such first-forbidden transitions the formulas for the decay probability are applicable with a sufficiently high degree of accuracy.

Table 3 – Characteristics of a number of allowed β-transitions lg *ft*

Decay	$Z_{mat} \rightarrow Z_{daught}$	$I_i^{\pi_i} \rightarrow I_f^{\pi_f}$	Type	E_0, keV	$T_{1/2}$	lg *ft*
$^{33}P \rightarrow ^{33}S$	15→16	$1/2^+ \rightarrow 3/2^+$	Allowed	249	25,3	5,0
$^{35}S \rightarrow ^{35}Cl$	16→17	$3/2^+ \rightarrow 3/2^+$	«»	167,4	days	5,0
$^{45}Ca \rightarrow ^{45}Sc$	20→21	$7/2^- \rightarrow 7/2^-$	Above	257	87,4	6,0
$^{63}Ni \rightarrow ^{63}Cu$	28→29	$1/2^- \rightarrow 3/2^-$	«»	65,8	days	6,6
$^{106}Ru \rightarrow ^{106}Rh$	44→45	$0^+ \rightarrow 1^+$	«»	39,4	165	4,3
$^{155}Eu \rightarrow ^{155}Gd$	63→64	$5/2^+ \rightarrow 3/2^+$	«»	140,7	days	7,4
$^{241}Pu \rightarrow ^{241}Am$	94→95	$5/2^+ \rightarrow 3/2^-$	First ban	20,8	100 days	5,8
					367 days	
					4,9 years	
					14,4 years	

In [3], the results of a test calculation of the probabilities and half-lives $T_{1/2}$ of a number of super-resolved beta transitions, in particular, $^{34}Cl \rightarrow ^{34}S$, $^{42}Sc \rightarrow ^{42}Ca$. Recall that for superallowed $\beta^{\pm}$-transitions $\int 1$ can be calculated exactly $\int 1 = [(T \pm T_3) \cdot (T \pm T_3 + 1)]^{1/2}$, where T_3 – isospin projection for the initial nucleus, numerically equal to ½ (Z – N).

If the β-transition occurs between pure isospin states, then taking into account the meson exchange currents (as a rule, contributing to a few percent) does not change this result, which is due to the conservation of isospin.

In the case of super-allowed transitions $0^+ \rightarrow 0^+$ between neighboring terms of the isomultiplet $\int \sigma = 0$ and, at T=1, $\int 1 = \sqrt{2}$. For such super-allowed transitions, the *f* $T_{1/2}$ values are almost the same.

The performed calculation (the well-known Gauss model was used to determine the charge distribution in the nucleus) gave the following values of the

half-lives for the transitions $^{34}Cl \rightarrow ^{34}S$ (1,55 s), $^{42}Sc \rightarrow ^{42}Ca$ (0,67 s). The sought data are in good agreement with the experimental values (respectively: 1,565±0,007 s; 0,683±0,002 s). For comparison, we present similar calculation data in the framework of the standard model of the Dirac-Fock atom (1,52; 0,64), as well as in the framework of the Hartree-Fock-Slater method (1,4; 0,6) [12,13]. Thus, in the approach proposed by us, it is more correct to take into account exchange-correlation and other effects. As you can see, the accuracy of calculations within the framework of the standard and optimized DF method is quite acceptable. It seems important to study in more detail the influence of the choice of the atomic field on the values of the Fermi function.

Results of computing an effect of an atomic field type choice on the beta decay characteristics. Further we present the results of evaluating the influence on the Fermi function of the choice of the type of atomic field, which is determined in different ways in different calculation methods. Note that in a number of works (see, for example, Refs. [2-13]) various methods were used to calculate the characteristics of beta decays, in particular, the method of the self-consistent nonrelativistic atomic field of the HFS, the method of the relativistic self-consistent field of the HFS (taking into account relativistic corrections in the Breit-Pauli approximation), the classical and improved versions of the Dirac-Fock method (ODF).

In order to compare different approaches, the calculation of the Fermi function *F(E,Z)* was carried out under conditions similar to [12,13], namely, in all cases the values of the functions on the boundary of the kernel $R_0 = 1{,}202\ A^{1/3}$ fm with the same A. The corresponding numerical results of the influence of the choice of the field (HFS_{rel}, HFS_{nonrel}, N-QED) on the Fermi function *F(E,Z)* for various beta decays are given in Tables 4, 5. The parameters were calculated as test values:

$$\Delta_1 = \{[\, F_{HFSrel}\ (E,Z) / F_{HFSnonrel}\ (E,Z)\,] - 1\} \cdot 100\%, \qquad (57a)$$

$$\Delta_2 = \{[\, F_{ODFrel}\ (E,Z) / F_{HFSnonrel}\ (E,Z)\,] - 1\} \cdot 100\%, \qquad (57b)$$

where F_{HFSrel} (E,Z) – Fermi function in atomic field HFS_{rel}; $F_{HFSnonrel}$ (E,Z) – Fermi function in atomic field HFS_{nonrel}; F_{ODFrel} (E,Z) – Fermi function in atomic field N-QED. Note also that in all three calculations, the effect of the finite size of the nucleus was taken into account within the framework of the model of a uniformly charged ball. As the calculation has shown, the use of the alternative

Gauss model has practically no effect on the results obtained, although it is more convenient computationally.

Table 4 - Effect on the Fermi function *F(E,Z)* for *β*-decay choice fields (HFS_{rel}, HFS_{nonrel}, ODF): values Δ_1 (%)

E_{kin}, keV	*Z*=20	*Z*=80	*Z*=95
10	-0,05	-0,34	-0,56
50	-0,03	-0.34	-0,55
100	+0,01	-0,34	-0,45
500	+0,08	-0,30	-0,40

Note. Here $\Delta_1 = \{[F_{HFSrel}(E,Z) / F_{HFSnonrel}(E,Z)] - 1\} \cdot 100\%$, where $F_{HFSrel}(E,Z)$ – Fermi function in atomic field HFS_{rel} [2,12]; $F_{HFSnonrel}(E,Z)$ – Fermi function in atomic field HFS_{nonrel} [2,3,12,13,18].

Table 5 - Effect on the Fermi function *F(E,Z)* for *β*-decay choice fields (HFS_{rel}, HFS_{nonrel}, ODF): values Δ_2 (%)

E_{kin}, keV	*Z*=20	*Z*=44	*Z*=63	*Z*=80	*Z*=95
10	-0,08	-0,10	-0,24	-0,56	-0,79
50	-0,06	-0,08	-0,23	-0.55	-0,77
100	+0,04	-0,07	-0,18	-0,54	-0,68
500	+0,13	-0,06	-0,14	-0,51	-0,61

Note. Here $\Delta_2 = \{[F_{ODFrel}(E,Z) / F_{HFSnonrel}(E,Z)] - 1\} \cdot 100\%$, where $F_{HFSnonrel}(E,Z)$ – Fermi function in atomic field HFS_{nonrel}; $F_{ODFrel}(E,Z)$ – Fermi function in atomic field N-QED [2,12,13].

Analysis of the data obtained shows that for small and medium values of the nucleus of the nucleus, in particular, Z = 20, the difference between the data obtained on the basis of the relativistic HFS and ODF methods turns out to be insignificant, amounting to hundredths of a percent. At large values of Z (up to Z = 95, calculations in the HFS_{rel} field gave a 0.5% lower value for *F(E,Z)*, and in the ODF field by 0,8%, in comparison with the nonrelativistic HFS_{nonrel} values. The reason for this difference is obviously related to the well-known effect of

relativistic compression of orbitals. The wave function of the continuous spectrum (continuum) is more screened from the charge of the atomic nucleus by the relativistic field of atomic electrons than by the nonrelativistic one, and the more accurately relativistic effects are taken into account, the greater the effect.

Results of computing the Fermi function of a β^--decay with different definitions of this function. Further, the difference in the values of the Fermi function *F(E,Z)* for the β^--decay is numerically estimated when choosing different definitions for the desired quantity. As indicated above, the Fermi function *F(E,Z)* was calculated by us both at the nuclear boundary and near zero. In the first case, the Fermi function *F(E,Z)* was calculated using the values of the radial electron wave functions $f^2_{+1}(R_0) + g^2_{-1}(R_0)$ – at the boundary of the nucleus (uniformly charged spherical nucleus), in the second, the Fermi function was calculated using the squared amplitudes of the expansion ($N^2_{\kappa=+1}+N^2_{\kappa=-1}$) radial electron wave functions $f^2_{+1}(0) + g^2_{-1}(0)$ at r→0 [2,12,13]. A convenient value characterizing the desired difference is the parameter:

$$\Delta_3 = \{[F(E,Z,R = 0)) / F(E,Z,R = R_0] - 1\} \cdot 100\%, \qquad (58)$$

where $F(E,Z,R=R_0)$ – Fermi function value calculated with values of radial electron wave functions at the nucleus boundary; $F(E,Z,R=0)$ – the value of the Fermi function calculated using the amplitudes of the expansion of the radial wave functions near zero.

The results of calculating the differences in the values of the Fermi function *F(E,Z)* for β-decay when choosing two different definitions of this quantity are given in the Table 6. The results of our calculation within the framework of the ODF method are presented, as well as for comparison for a number of values of the kinetic energy the data of estimates within the framework of the relativistic HFS (e.g.[12,13]). Analysis of the results shows that with an increase in the atomic number Z, the difference in the values of the Fermi function determined by different methods sharply increases. The change in the integral Fermi function $f(E_0,Z)$ turns out to be similar. In particular, the calculation showed that the function *f* increases for decays $^{33}P \rightarrow ^{33}S$ (E_0 = 249 keV), $^{35}S \rightarrow ^{35}Cl$ (E_0=167 keV) by 2-4%, $^{63}Ni \rightarrow ^{63}Cu$ (E_0=65,8 keV) – 5%, $^{155}Eu \rightarrow ^{155}Gd$ (E_0=140,7 keV) – 12%, $^{241}Pu \rightarrow ^{241}Am$ (E_0=20,8 keV) – 32% (when passing from the definition of *F(E,Z)* by functions at

Table 6 - The difference in the Fermi function *F(E,Z)* for *β*-decay when choosing different definitions for this quantity: $\Delta_3=\{[F(E,Z,R=0))/F(E,Z,R=R_0]-1\}\cdot 100\%$, where $F(E,Z,R=R_0)$ calculated with the values of radial electron wave functions at the nucleus boundary, and $F(E,Z,R=0)$ – using the amplitudes of the expansion of the radial wave functions near zero ($R_0 = 1{,}2\ A^{1/3}$ fm); HFS – work data [12,13]; N-QED – calculation data within the framework of the N-QED theory (e.g.[2,3,5,12,13,18])

E_{kin}, keV	Δ_3, %					
	Z=20		*Z*=44	*Z*=63	*Z*=80	*Z*=95
	HFS	N-QED				HFS N-QED
0,1	1,35	1,39	5,44	12,72	23,25	33,9
1,0	1,37	1,42	5,53	12,84	23,36	36,8
50	1,38	1,45	5,58	12,95	23,58	34,1
500	1,50	1,58	5,84	13,10	24,61	37,2
						34,2
						37,6
						35,5
						39,88

the boundary of the kernel to the definition of *F(E,Z)*, calculated from the amplitudes at zero).

Note that in the literature there have been various points of view on the correctness and acceptability of one or another approach to the definition of the Fermi function.

In our opinion (see also [2,3,5,12]), the determination of the Fermi function using the amplitudes of the expansion of wave functions near zero is more justified and rational. As indicated in [2,12,13,18], an additional factor in favor of this statement is the fact that, based on the amplitudes of the expansion of the electronic wave functions at zero, one usually calculates, for example, the electronic factor of the EO conversion Ω(EO), corrections to the internal conversion coefficients to take into account anomalies etc.

Let us now consider the question of the region of formation of the integral Fermi function $f(E_0,Z)$. A convenient parameter for this estimate is the quantity used in a number of works (see, for example, [2,12]):

$$y = \int_0^x F(E,Z)\, Ep\, (E_0 - E)^2\, dE \,/\, \int_0^{E_0} F(E,Z)\, Ep\, (E_0 - E)^2\, dE. \qquad (59)$$

Table 7 shows our calculated data on the formation region of the integral Fermi function $f(E_0,Z)$ for a series of β-decays, in particular, decays: $^{241}Pu \rightarrow ^{241}Am$, $^{106}Ru \rightarrow ^{106}Rh$, $^{63}Ni \rightarrow ^{63}Cu$, $^{155}Eu \rightarrow ^{155}Gd$, $^{35}S \rightarrow ^{35}Cl$, $^{33}P \rightarrow ^{33}S$, $^{45}Ca \rightarrow ^{45}Sc$.

Analysis of the data obtained (Table 7) shows that for energy values from $x=0,7E_0$ and further to $x=0,9E_0$, 100% of the integral for the function $f(E_0,Z)$. At an energy value x = $0,5E_0$, about ~ 80% of the integral for the function $f(E_0,Z)$.

As a result, it turns out that the corrections, which are significant for small values of the energy of the emitted β-particle, affect the integral Fermi function. Next, we will study the question of the quantitative characteristic of taking into account the exchange-correlation effects in the wave functions of the discrete and continuous parameters of the Fermi functions.

Table 7 – Formation region of the integral Fermi function $f(E_0,Z)$ for β-decay (our data)

E_0, keV	β-decay	y, %			
		x/E_0 =0,3	0,5	0,7	0,9
20,8	$^{241}Pu \rightarrow ^{241}Am$	67	89	99	100
39,4	$^{106}Ru \rightarrow ^{106}Rh$	66	88	98	100
65,8	$^{63}Ni \rightarrow ^{63}Cu$	65	87	97	100
140,7	$^{155}Eu \rightarrow ^{155}Gd$	63	84	96	100
167,4	$^{35}S \rightarrow ^{35}Cl$	58	81	95	100
249	$^{33}P \rightarrow ^{33}S$	53	78	93	100
257	$^{45}Ca \rightarrow ^{45}Sc$	52	77	91	100

Further consider an effect of accounting the exchange-correlation effects in wave functions on the values of the integral Fermi function. The nuclear QED approach developed by us allows for a full account of exchange effects, as well as correlation effects.

In this subsection, we quantitatively study the influence of taking into account the sought effects in the electronic wave functions on the values of the

Fermi function and the integral Fermi function. It should be noted that the issue of accounting for exchange was considered earlier in the literature (see, e.g., [2,3,5,12,13,18]).

The study of the contribution of correlation effects is considered here for the first time.

Table 8 shows the results of calculating the contribution of the value of complete accounting for exchange in the electronic wave functions of discrete and continuous spectra to the values of the integral Fermi function $f(E_0,Z)$; on the basis of various approaches [2,3,5,12,13,18], transitions are considered: $^{35}S \rightarrow ^{35}Cl$, $^{63}Ni \rightarrow ^{63}Cu$, $^{33}P \rightarrow ^{33}S$, $^{106}Ru \rightarrow ^{106}Rh$, $^{155}Eu \rightarrow ^{155}Gd$, $^{241}Pu \rightarrow ^{241}Am$. As a convenient parameter that determines the desired contribution, we took the quantity:

$$\Delta_4 = \{[\, f(E_0,Z)ODF / f(E_0,Z]\, HFS_{rel}) \,]\text{-}1\} \cdot 100\%, \qquad (60a)$$

$$\Delta_5 = \{[\, f(E_0,Z)DF / f(E_0,Z]\, HFS_{rel}) \,]\text{-}1\} \cdot 100\%, \qquad (60b)$$

where $f(E_0,Z)ODF$ – integral Fermi function calculated in the N-QED approximation with full allowance for exchange-correlation effects; $f(E_0,Z)DF$ – integral Fermi function calculated in the DF approximation with full allowance for exchange effects; $f(E_0,Z]HFS_{rel})$ – integral Fermi function calculated in the HFS_{rel} approximation with incomplete account of exchange effects. As the DF of the used results of our calculation, taking into account the exchange-correlation effects (Δ_4), and also for comparison of the classical DF-calculation of the Band-Listengarten-Trzhaskov (Δ_5) taking into account exchange effects [12,13]).

As can be seen from the data obtained, with an increase in the completeness of accounting for exchange (and further exchange-correlation) effects in the wave functions of the discrete and continuous spectrum, the correction to the energy increases with a decrease in the boundary energy. The relative change in the integral Fermi function, for example, for the $^{241}Pu \rightarrow ^{241}Am$ transition is 7,6%.

Further consider an effect of accounting the exchange-correlation effects in wave functions on the values of the Fermi function. Let us note that the question of the influence of taking into account exchange-correlation effects in the wave functions of the discrete and continuous spectrum on the values of the Fermi function is of a great importance.

Table 8 – Contribution of the value of the complete account of exchange in the electronic wave functions of discrete and continuous spectra to the values of the integral Fermi function $f(E_0,Z)$ for some transitions

Decay	E_0, keV	$f(E_0,Z)$ ODF	$f(E_0,Z)$ DF	$f(E_0,Z)$ HFS_{rel}	Δ_4, %	Δ_5, %
$^{35}S\rightarrow^{35}Cl$	167,4	$1{,}3461\cdot10^{-2}$	$1{,}3556\cdot10^{-2}$	$1{,}3682\cdot10^{-2}$	-1,6	-0,9
$^{106}Ru\rightarrow^{106}Rh$	39,4	$6{,}2375\cdot10^{-4}$	$6{,}4304\cdot10^{-4}$	$6{,}6304\cdot10^{-4}$	-5,9	-3,0
$^{155}Eu\rightarrow^{155}Gd$	140,7	$8{,}6124\cdot10^{-2}$	$8{,}7025\cdot10^{-2}$	$8{,}8817\cdot10^{-2}$	-3,0	-2,0
$^{241}Pu\rightarrow^{241}Am$	20,8	$1{,}5896\cdot10^{-3}$	$1{,}6424\cdot10^{-3}$	$1{,}7208\cdot10^{-3}$	-7,6	-4,6

Note: Here $\Delta_4=\{[f(E_0,Z)ODF / f(E_0,Z]\ HFS_{rel})]-1\}\cdot100\%$, where $f(E_0,Z]HFS_{rel})$ – integral Fermi function calculated in the HFS_{rel} approximation with incomplete account of exchange effects; $\Delta_5 = \{[\ f(E_0,Z)DF\ /\ f(E_0,Z]\ HFS_{rel})]-1\}\cdot100\%$, where $f(E_0,Z)DF$ – integral Fermi function calculated in the DF approximation with full account of exchange (exchange-correlation) effects.

Table 9, 10, 11 shows the data of our calculation of the values of the Fermi function $F(E,Z)$ for decays: $^{106}Ru\rightarrow^{106}Rh$, $^{63}Ni\rightarrow^{63}Cu$, $^{241}Pu\rightarrow^{241}Am$. For comparison, the same table also shows some values of the function $F(E,Z)$, calculated by the HFS_{rel} method, by the DF method, as well as in the Coulomb field approximation, taking into account the finite dimensions of the nucleus (data taken from [2,3,5,12,13,18]).

As characteristic parameters determining the contribution of the sought effects, it is convenient to operate with the quantities:

$$\Delta_6 = \{[F(E,Z)QED / F(E,Z]HFS_{rel})]-1\}\cdot 100\%, \qquad (61a)$$

$$\Delta_7 = \{[F(E,Z)DF_{exc} / F(E,Z]HFS_{rel})]-1\}\cdot 100\%, \qquad (61b)$$

$$\Delta_8 = \{[F(E,Z)HFS_{rel})/ F(E,Z)_{Coulomb})-1)\cdot 100\%, \qquad (61c)$$

Table 9 - The functions $F(E,Z)$ and the influence on it of the complete accounting for exchange (correlation) in the wave functions of the DF of discrete and continuous spectra (transition: $^{106}Ru\rightarrow^{106}Rh$)

E_{β^-} kin, keV	Z=45	$F(E,Z)$ ^{106}Ru→^{106}Rh; E_0 = 39,4keV			- Δ_6, %	- Δ_7, %	- Δ_8, %
	QED_{exc}	DF_{exc}	HFS_{rel}	Coulomb			
0,5140	84,0896	86,3579	93,6620	95,3163	10,2	7,8	1,7
2,6582	38,7468	39,6767	41,2162	42,0030	6,0	3,7	1,9
6,3456	25,6138	26,1625	26,8605	27,3434	4,6	2,6	1,8
16,767	16,0979	16,3667	16,6530	16,9466	3,3	1,7	1,7
28,233	12,6722	12,7921	12,9745	13,2067	2,3	1,4	1,8
39,314	10,8742	10,9863	11,1218	11,3237	2,2	1,2	1,8

Table 10 – The Fermi function *F(E,Z)* and the effect on it of a complete account of the exchange (correlation) in the wave functions of the DF of discrete and continuous spectra (transition: ^{63}Ni→^{63}Cu)

E_{β^-} kin, keV	$F(E,Z)$ ^{63}Ni→^{63}Cu; Z=29; E_0 = 65,8 keV			Δ_6, %	Δ_8, %
	QED_{exc}	HFS_{rel}	Coulomb		
0,85858	29,3482	31,5491	31,8710	-7,0	-1,0
4,4394	13,4120	13,9167	14,0385	-3,6	-0,9
10,547	8,8125	9,0867	9,1751	-3,0	-1,0
28,002	5,6139	5,7411	5,8094	-2,2	-1,2
47,159	4,5391	4,6076	4,6644	-1,5	-1,2
65,657	4,0197	4,0652	4,1132	-1,1	-1,2

where $F(E_0,Z)QED_{exc}$ – Fermi function calculated in the optimized approximation N-QED with full account of exchange-correlation effects; $F(E_0,Z)DF_{exc}$ – Fermi function calculated in the DF approximation with full allowance for exchange effects; $F(E_0,Z]HFS_{rel})$ – Fermi function calculated in the HFS_{rel}

approximation with incomplete account of exchange effects; $F(E,Z)_{Coulomb}$ – Fermi function (Coulomb approximation).

As can be seen from the data obtained (see Tables 9-11), the correction associated with taking into account the exchange-correlation effects in the electronic wave functions of the discrete and continuous spectra at low energies significantly exceeds the correction for screening (with respect to the Coulomb field), which is found using the HFS_{rel} method, however, with increasing energy, the screening correction is gradually compared with the exchange contribution.

It is easy to understand that the construction of the Curie plot according to our calculated data *F(E,Z)*, as well as according to the data of the standard DF calculation (e.g. [2,3,5,12,13,18], in comparison with similar data based on the HFS_{rel} method, in the region of low energy values will have excess over a straight line drawn through points with higher energy.

Table 11 – Fermi function *F(E,Z)* and the influence on it of the complete account of exchange (correlation) in the wave functions of the DF of discrete and continuous spectra (transition: $^{241}Pu \rightarrow ^{241}Am$)

E_{β^-} kin, keV	Z=95	*F(E,Z)* $^{241}Pu \rightarrow ^{241}Am$; E_0 = 20,8 keV			$\Delta_{6,}$ %	$\Delta_{7,}$ %	$\Delta_{8,}$ %
	QED_{exc}	DF_{exc}	HFS_{rel}	Coulomb			
0,27137	2014,27	2075,86	2316,49	2431,60	-	-	-4,7
1,4033	944,400	961,517	1018,29	1069,57	13,0	10,4	-4,8
3,3341	621,735	634,238	661,040	694,165	-7,3	-5,6	-4,0
8,8517	391,342	394,909	406,591	426,528	-5,9	-4,1	-4,7
14,907	303,169	306,220	313,858	329,084	-3,8	-2,9	-4,6
20,755	259,003	260,587	266,528	279,230	-3,4	-2,4	-4,5
					-2,8	-2,2	

Then, such an excess can simulate a massive neutrino with a nonzero mass in the amount of 1,8% of the number of decays.

1.5 Conclusions

We have briefly presented the modern concepts of physical nature of a beta-decay and considered the key fundamental parameters of a nuclear beta-decay, classification of the beta-transitions, selection rules etc. An effective relativistic approach to calculating the characteristics of the β-decay for different of atomic systems (nuclei) is presented and based on the combined relativistic nuclear model and relativistic many-body perturbation theory formalism with correct accounting for exchange-correlation, nuclear, radiation corrections. A relativeistic many-body perturbation theory is applied to electron subsystem, and a nuclear relativistic middle-field model is used for nuclear subsystem. The results of computing the characteristics of a whole series of allowed (super-allowed) β-decays are presented, namely, for the $^{33}P \rightarrow ^{33}S$, $^{35}S \rightarrow ^{35}Cl$, $^{45}Ca \rightarrow ^{45}Sc$, $^{63}Ni \rightarrow ^{63}Cu$, $^{106}Ru \rightarrow ^{106}Rh$, $^{155}Eu \rightarrow ^{155}Gd$, $^{241}Pu \rightarrow ^{241}Am$ decays. The effect of the chemical environment of an atom on the characteristics (integral Fermi function, half-life) of β-transitions is studied. We presented the results of accurate calculation of the beta-decay parameters and compared with alternative theoretical data. Results of computing the Fermi function of a β^--decay with different definitions of this function are presented too. The effect of an atomic field type choice on the beta decay characteristics as well as the influence of accounting for the exchange-correlation effects in the wave functions of the discrete and continuous spectrum on the values of the Fermi and integral Fermi functions are calculated.

PART II RELATIVISTIC QUANTUM CHEMISTRY AND SPECTROSCOPY OF SOME KAONIC ATOMS: HYPERFINE AND STRONG INTERACTION EFFECTS

Abstract. We present a consistent relativistic approach to calculation of energy and spectral parameters of the kaonic exotic atomic systems with accounting for the nuclear radiative (quantum electrodynamics), hyperfine and strong interactions. The approach is naturally based on using the relativistic Klein-Gordon-Fock equation with introduction of electromagnetic and strong interactions potentials. To take a strong kaon-nuclear interaction into account, the generalized optical potential method is applied. In order to take the nuclear (the finite nuclear size effect) and radiative (quantum electrodynamics) corrections into account, the generalized Uehling-Serber approach is applied. The elements of the hyperfine structure theory of the kaonic atoms (KA) are presented. As an illustration, there are results of calculating the binding energies of various atomic levels in a hydrogen KA obtained within the H-like model of Iwasaki, the method of Indelicato et al and our approach (here the Fermi model of the charge distribution in the nucleus is used). Using our calculated "electromagnetic" values of the transition energy and a set of available latest experimental values, it is calculated a shift of the 1s level in kaonic hydrogen, due to the strong kaon-nucleon interaction; the calculated "electromagnetic" value of the transition energy and further comparison with the experimental value of the transition allowed to obtain a theoretical estimate of the "strong" shift in kaonic hydrogen, which is in excellent agreement with the DEAR experimental data. In addition, the results of calculating the energy (electromagnetic) contributions (the main Coulomb correction, correction for vacuum polarization, relativistic correction for the recoil effect, a hyperfine shift) to the energy of the 8k-7i, 8i-7h transitions in the spectrum of kaonic nitrogen are presented and compared with the alternative theoretical data by Indelicato et al. .

Keywords: Quantum mechanics and spectroscopy - Kaonic atoms - Relativistic many-body perturbation theory - Klein-Gordon-Fock equation -Strong kaon-nuclear optical potential - Hyperfine Structure

2.1 Introduction

At present, an exotic atom is usually understood as a bound or quasi-stationary complex, which is obtained as a result of the landing of a heavy negatively charged particle (hadron, lepton) X $\left(X=\mu^{-},\pi^{-},K^{-},p^{-},\Sigma^{-},...\right)$ on an ordinary atom [1-50]. Hence the name of various types of exotic atoms, in particular, pionic, hyperonic, and KA of interest to us. Antihydrogen $\left(p^{-}e^{-}\right)$, muonium $\left(\mu^{-}e^{-}\right)$, and other systems are sometimes referred to such systems. The progress observed in the last decade in the theoretical and experimental study of hadronic atoms has been noted in a number of rather interesting reviews both on the physics of KA and on the physics of other hadronic atoms (see, for example, [51-60]).

Despite the more than 70-year period of the development of the physics of hadronic atoms, until the early 2000s, the situation with the data on the energy parameters of most kaonic, pionic, and other atoms was rather confusing [1-50]. Moreover, in recent years, the situation in the physics of kaonic atoms (KA) continues to change rapidly, the most striking example of which is the recent solution to the problems of kaonic hydrogen and helium (see [1-4] and the text below), due, among other things, to huge experimental errors. The study of kaonic atoms has become especially relevant in the light of the well-known progress of experimental studies (at meson factories in the laboratories of LAMPF (USA), PSI (Switzerland), TRIUMF (Canada), IFF (Russia), RIKEN (KEK, Japan), RAL (United Kingdom), DEAR at the DAPNE (Italy) and further substantial development of modern nuclear theory, quantum mechanics of atoms etc. At present, it is customary to consider (see, e.g., [1-10]) that the main tasks of modern physics of the nucleus, elementary particles and high energies are to check the consequences and search for violations of the Standard Model of electroweak interactions with the aim of generalizing it, determining the neutrino masses, elucidating cosmological consequences from the physics of the microworld, etc.

Experimental studies here, as a rule, are developing in two complementary directions, in particular, the basis of the first is the construction of high-energy accelerators and unique detectors in order to detect new particles and interactions and verification of theoretical models [1-56]. The second direction is precisely the physics of hadronic atoms or, as is often indicated, the physics of intermediate energies, including the determination of the energy and spectral parameters of systems, as well as the search for rare decays and reactions with al-

ready known particles, the detection of violations of the fundamental properties of symmetry, the study of atomic and molecular processes with the participation of hadronic, including kaonic atoms.

It should be noted that the most correct approach to description of the kaonic atomic systems should be based on the principles of a modern consistent quantum chromodynamics with some elements of a quantum electrodynamics in a case of multielectron kaonic atoms. One could remind that consistent quantum chromodynamics represents a fundamental gauge theory of strong interactions with the interacting coloured quarks and gluons. Due to the strong interaction effect, there is a shift of energies of the low-lying levels from the purely electromagnetic values and the finite lifetime of the state corresponds to an increase in the observed level width. A few serious measurements are performed for different light and heavy kaonic atoms (e.g. [1-5]).

The most spread theoretical methods to study energy and spectral characteristics of kaonic atomic systems are described in Refs. [1-56]. In Refs. [43-56] ab initio schemes to the Klein-Gordon-Fock equation solution and further determination of the X–ray spectra for multi-electron kaonic atoms are presented with the different procedure for accounting for the nuclear, quantum electrodynamics, interelectron and kaon-electron interaction, exchange-correlation effects.

Another extremely fundamental aspect of the theory of hadronic atoms, in particular, KA, is associated with taking into account the radiation, QED corrections to the energy of the atom (transition energies, etc.) [57-74]. First of all, we are talking about taking into account the effect of vacuum polarization, as well as the less significant contribution for KA, due to the self-energy part of the Lamb shift. In [1,4, -, 5 42,43,57-78], a review of the current state of calculating radiative corrections to the energies of levels in kaonic atoms is given, and existing problems are analyzed, in particular, the difficulties of calculating the required radiative corrections in the case of heavy systems.

For a point nucleus in the first order of PT in $Z\alpha$ (Z is the nuclear charge; α is the fine structure constant), the vacuum polarization addition to the nucleus potential is the known Uehling-Serber potential $\tilde{U}(r)$. Taking into account the finiteness of the size of the nucleus modifies this potential. In the well-known works of Wichmann-Kroll (see [1,42,43,57-74]), a method was developed that makes it possible to calculate the vacuum polarization in all orders by $\alpha\ (Z\alpha)^n$. In principle, the polarization shift could be calculated as a first-order correction to the potential $\tilde{U}(r)$. Convenient techniques with application to the description of the spectra of ordinary heavy atoms and multiply charged ions have been pro-

posed and implemented in the papers by Declaux -Indelicato, Mohr, Saperstein, Johnson et al (see, for example, [1-4,50-98]). However, it should be noted that the main techniques based on the expansion of the contribution of radiative corrections by $z\alpha$, naturally, work only for systems with low Z, i.e., light atoms. In the case of heavy systems, in particular, KA, these approaches will obviously not give correct results.

In Ref. [2, 81,82,91,92] we have presented an effective relativistic approach to calculation of spectra and the spectroscopic properties of the heavy kaonic (pionic) multielectron atomic systems. The approach is based on the Klein-Gordon-Fock equation solution with simultaneous accounting for electromagnetic and strong kaon-nuclear interactions.

The modified method of optical potential is used to take a strong kaon-nuclear interaction into consideration. The consistent procedures, in particular, such as an advanced Uehling-Serber model and model potential approach are applied to take the main nuclear and quantum electrodynamics corrections into account. The results of calculation of the energy and spectral parameters for the kaonic atoms of He, ^{184}W, ^{207}Pb, ^{238}U, with taking the radiation (vacuum polarization), nuclear (finite size of a nucleus) and the strong kaon-nuclear interaction corrections into account have been presented. In this chapter we present the generalization of theory in order to determine the hyperfine and strong interaction effects as well as to calculate the probabilities of the radiative transitions in spectra of the hydrogen (including the kaonic hydrogen puzzle) and nitrogen kaonic atoms.

2.2 Relativistic theory of kaonic atoms with accounting for the nuclear, hyperfine and strong interaction effects

2.2.1 The Klein-Gordon-Fock equation and electromagnetic interactions in kaonic system

New version of a relativistic theory of kaonic atomic systems with accounting for the nuclear, radiation, hyperfine and strong interaction effects has been in detail presented in Refs. [2, 81,82,91,92]. So, here it is worth to consider only some new model elements. However, at once, we present shortly the summary of modern kaon data [1-10].

There are 4 types of kaons: negatively charged K^- (composition: s-quark + u-antiquark), m_{K^-}=493.667±0.013 MeV; lifetime ((1.2384±0.0024)10^{-8} sec and radius: r_{K^-}=0.560±0,031fm. Its antiparticle is a positively charged kaon K^+ (composition: u-quark + s-antiquark). Naturally, due to the CPT symmetry, $m_{K^+}=m_{K^-}$, $t=t_{K^-}$ should take place (modern data: Δm=0.032±0.090 MeV; Δt=(0.11±0.09)10^{-8}sec). Neutral kaons $K^0, \tilde{K}^0$ have the following composition: d-quark + s-antiquark and s-quark + d-antiquark, m_{K^o}=497.648±0.022 MeV. Since K^0 and the antiparticle $\tilde{K}^0$ appear as a result of strong interaction, they decay due to weak interaction and represent a composition of 2 weak eigenstates: short-lived neutral $K=K_S$ ("K-short"; decays into 2 pions and t_{K^o}= 8.958×10^{-11} sec) and long-lived neutral $K=K_L$ ("K-long"; decays into 3 pions and t_{K^o}= 5.18×10^{-8} sec).

The kaonic wave functions are determined from solution of the known relativistic Klein-Gordon-Fock equation:

$$\{\frac{1}{c^2}[E+eV_0(r)]^2+\hbar^2\nabla^2-m^2c^2\}\varphi(x)=0 \qquad (1)$$

Here c is a velocity of light, E is the total energy of atomic system, V_0 is a sum of electric potential of a nucleus and strong interaction potential and the Uehling-Serber potential. To determine the electric potential of the nucleus, we used the Fermi model with charge distribution $\rho(r)$ [1]:

$$\rho(r)=\rho_0/\{1+\exp[(r-c)/a)]\} \qquad (2)$$

where parameter $a=0.523$ fm, and parameter c is chosen so that the root-mean-square radius is determined by the expression: $<r^2>^{1/2}=(0.836\cdot A^{1/3}+0.5700)$ fm. As an alternative, as usual in atomic calculations, the empirically determined Z-dependence for the effective radius is used [1].

Other versions of the nuclear electric potential are presented by the Gauss and a homogeneously charged sphere models [92, 93]. The standard point of our theoretical approach is connected with determination of the electric and radiative potentials within the effective algorithm based on the differential equations method. This is the method originally developed by Ivanova and Ivanov [86] and further has been often used in solving many problems of atomic, molecular, nuclear and laser spectroscopy (e.g. [1,38,39,86,87,99-

140]). It is important to underline too that in order to determine an electrical interaction between a nucleus of finite size (radius of R_1) and kaon (radius R_2), one should use, for example, the potential, introduced by Indelicato et al [42,43,50] (e.g. Refs. [2, 81,82,91,92] too).

The next principally important block of our approach includes an accurate treatment of the radiative (quantum electrodynamics) effects (e.g., [37-41,57-68, 86-90]). We have used an effective the generalized Uehling-Serber approach to accounting the radiative corrections, in particular, vacuum-polarization one. The standard Uehling-Serber potential can be written as follows:

$$U(r) = -\frac{2\alpha}{3\pi r}\int_1^\infty dt \exp(-2rt/\alpha Z)(1+1/2t^2)\frac{\sqrt{t^2-1}}{t^2} \equiv -\frac{2\alpha}{3\pi r}C(g),$$

$$g = r/\alpha Z \qquad (3)$$

where α-constant of fine structure, which in fact (even taking into account the finite size of the nucleus) takes into account the main contributions of the order $[\alpha\,(Z\alpha)]^n$, but does not take into account the known contributions of Källen-Sabry, Wichmann-Kroll and others.

A more correct form of the Uehling-Serber potential is

$$U(r)=-(2\alpha/3\pi r)C(g),$$

where C is the so-called Uehling-Serber integral, but as $C(g)$ the generalized function e.g. [1, 37-40, 86-90]) is used and then performed the transition from the potential U for the point core to the potential for the finite core.

To take into account the effect of electron shielding (in the case of the nitrogen atom), the usual potential of a self-consistent electron field is used.

The whole procedure of accounting for the QED corrections is in detail described in Refs. [1,85-87,91-93] as well as the fine corrections, provided by relativistic recoil, reduced mass and other effects.

Further in order to calculate the radiation transition probabilities or a radiation width in spectra of the kaonic atom we apply our traditional relativistic energy formalism in the version [37-39,66,67,85-87].

A total energy level shift δE can be presented in the following form:

$$\delta E_i = \mathrm{Re}\,\delta E_i + i\,\mathrm{Im}\,\delta E_i = \mathrm{Re}\,\delta E_i - (i/2)\Gamma_i^r\,, \qquad (4)$$

where Γ_i^r is a level radiation width. It should be noted that an oscillator strength (or transition probability) is directly connected with Γ_i^r ($P_i \sim \Gamma_i^r$) and further is determined by combination of amplitudes $<ij|\sin(i\,|\,\omega\,|\,r_{ij})/r_{ij}\,|\,ji>$ (ω_{ij} is a frequency of the *i-j* transition). The detailed procedure for computing the radiative transition matrix elements as well as the hyperfine structure characteristics is presented in Refs. [1,48-50,66,67,72-77,88,90]. All computing is carried out with using the PC code Superatom (version 98).

2.2.2 Model approach to study of the strong and hyperfine interactions in kaonic atoms

As it is indicated, the most correct approach to description of the kaonic atomic systems should be based on the principles of a modern consistent quantum chromodynamics with some elements of a quantum electrodynamics in a case of multielectron kaonic atoms. Indeed a quantum chromodynamics represents a fundamental gauge theory of strong interactions with the interacting coloured quarks and gluons.

From the other side, since we are interested by relatively low energy physics of the kaonic atomic systems, one should use different model potential methods to determine the strong kaon-nuclear interaction in these systems (e.g. [1-56]). In this case the total Klein-Gordon-Fock equation taking into account the strong kaon-nuclear interaction V_N can be written as follows:

$$\left[\hbar^2\nabla^2 + c^{-2}\left(E - V_{FS}\right)^2 - \mu^2 c^2\right]\psi = 2\mu V_N \psi\,. \qquad (5)$$

where the standard phenomenological optical potential with the proton ρ_p and neutron ρ_n densities is written taken as follows [45]:

$$V_N = -\frac{2\pi}{\mu}[1 + \frac{M_K}{M_N}][A_{Kp}\rho_p(r) + A_{Kn}\rho_n(r)]\,, \qquad (6)$$

All the parameters of the potential (6) are described in Refs. [45,51-53]).

As it is noted in Ref. [1], the key disadvantage of the used potential (5) approach is connected with inaccurate determination of its parameters, including the proton and neutron densities, the effective K-nucleon scattering lengths (e.g., Refs. [1,45,51-53]).

It should be noted that if the experimental value of energy $E_{\exp}$ is known, then one could easily calculate a strong kaon-nucleus interaction shift of the energy levels:

$$E_N = E_{\exp} - (E_{KGF} + E_{FS} + E_{QED} + \Delta E), \tag{7}$$

In Eq. (7) in the brackets different purely electromagnetic contributions (respectively, an energy of kaon in a case of point nucleus, the nuclear finite size and QED effects terms).

. The nuclear potential for the spherically symmetric density $\rho(r|R)$ can be presented as follows:

$$V_{nucl}(r|R) = -\left((1/r)\int_0^r dr' r'^2 \rho(r'|R) + \int_r^\infty dr' r' \rho(r'|R)\right) \tag{8}$$

Further the density can be approximated by the Gaussian function:

$$\rho(r|R) = \left(4\gamma^{3/2}/\sqrt{\pi}\right)\exp\left(-\gamma r^2\right) \tag{9}$$

$$\int_0^\infty dr r^2 \rho(r|R) = 1,$$

$$\int_0^\infty dr r^3 \rho(r|R) = R,$$

(here $\gamma=4/\pi R^2$ and R is the effective nucleus radius) or by the Fermi function:

$$\rho(r) = \rho_0 / \{1 + \exp[(r-c)/a)]\}, \tag{10}$$

where the parameter a=0.523 fm, the parameter c is chosen by such a way that it is true the following condition for average-squared radius:

$$<r^2>^{1/2}=(0.836\cdot A^{1/3}+0.5700)\text{fm}. \quad (11)$$

Further one should use the formulas for the finite size nuclear potential and its derivatives on the nuclear radius. Here we use the known Ivanov-Ivanova et al method of differential equations (look details in Refs. [80-83]). The effective algorithm for definition of the potential $V_{nucl}(r|R)$ is used in Refs. [65,72] and reduced to solution of the following system of the differential equations (for the Fermi model):

$$V'nucl(r,R)=\left(1/r^2\right)\int_0^r dr'\,r'^2\rho\left(r',R\right)\equiv\left(1/r^2\right)y(r,R),$$
$$y'(r,R)=r^2\rho(r,R), \quad (12)$$

$$\rho'(r)=(\rho_0/a)\exp[(r-c)/a]\{1+\exp[(r-c)/a)]\}^2$$

with the corresponding boundary conditions. In a case of the Gaussian model the corresponding system of differential equations is as follows:

$$V'nucl(r,R)=\left(1/r^2\right)\int_0^r dr'\,r'^2\rho\left(r',R\right)\equiv\left(1/r^2\right)y(r,R) \quad (13)$$
$$y'(r,R)=r^2\rho(r,R) \quad (14)$$

$$\rho'(r,R)=-8\gamma^{5/2}\,r/\sqrt{\pi}\exp\left(-\gamma r^2\right)=-2\gamma r\rho(r,R)=-\frac{8r}{\pi r^2}\rho(r,R) \quad (15)$$

with the boundary conditions:

$$V_{nucl}(0,R)=-4/(\pi r),$$

$$y(0,R)=0,$$

$$\rho(0,R)=4\gamma^{3/2}/\sqrt{\pi}=32/R^3 \quad (16)$$

Another, probably, more consistent approach is in using the relativistic mean-field (RMF) model, which been designed as a renormalizable meson-field theory for nuclear matter and finite nuclei [47].

The detailed procedure for computing the strong interaction corrections is presented in Refs. [1,48-50,66,67,72-77,88,90]. All computing is carried out with using the PC code Superatom (version 98).

2.3 Quantum electrodynamics effects in pionic atomic systems

Consistent and accurate account of the radiation or QED effects is of a great importance and interest in spectroscopy of the pionic atomic systems. To take into account the radiation (QED) corrections, namely, the important effect of the vacuum polarization one could use the procedure, which is in details described in the Refs. [41-58, 65,72-78].

Figure 1 [13] illustrates Feynman diagrams, which describe a QED effect of the vacuum polarization: A1 – the Uehling-Serber term; A2, A3 – terms of order $[\alpha\,(Z\alpha)]^n$ (n=2,..); A4- the Källen-Sabry correction of order $\alpha^2(\alpha Z)$; A5 –the Wichmann-Kroll correction of order κa $\alpha\,(Z\alpha)^n$ (n=3). An effect of the vacuum polarization is usually taken into account in the first PT theory order by means of the generalized Uehling-Serber potential with modification to take into account the high-order radiative corrections. In particular, the generalized Uehling-Serber potential can be written as follows:

$$U(r) = -\frac{2\alpha}{3\pi r}\int_1^\infty dt\,\exp\left(-2rt/\alpha Z\right)\left(1+1/2t^2\right)\frac{\sqrt{t^2-1}}{t^2} \equiv -\frac{2\alpha}{3\pi r}C(g), \qquad (17)$$

where

$$g = r/(\alpha Z).$$

More correct and consistent approach is presented in Refs. [42,43,52-62,134-160].

An accounting of the nuclear finite size effect modifies the potential (7) as follows:

$$U^{FS}(r) = -\frac{2\alpha^2}{3\pi}\int d^3r'\int_m^\infty dt\,\exp\left(-2t|r-r'|/\alpha Z\right)\times\left(1+\frac{1}{2t^2}\right)\frac{\sqrt{t^2-1}}{t^2}\frac{\rho(r')}{|r-r'|}, \qquad (18)$$

The Uehling-Serber potential, determined as a quadrature (11), may be approximated with high precision by a simple analytical function. The use of new approximation of the Uehling potential permits one to decrease the calculation errors for this term down to 0.5 – 1%.

A method for calculation of the self-energy part of the Lamb shift is based on an idea by Ivanov-Ivanova (see Ref. [80,81]), which generalizes the known hydrogen-like method by Mohr and radiation model potential method by Flambaum-Ginges (look details in Refs. [41,52,61,62]).

According to Ref. [9], in an atomic system the radiative shift and the relativistic part of energy are, in principle, defined by one and the same physical field. One could suppose that there exists some universal function that connects the self - energy correction and the relativistic energy. The self-energy correction for the states of a hydrogen-like ion was presented by Mohr [41] as:

$$E_{SE}\left(H|Z,nlj\right)=0.027148\,\frac{Z^4}{n^3}\,F\left(H|Z,nlj\right) \qquad (19)$$

The values of F are given at $Z=10-110,\ nlj=1s,2s,2p_{1/2},2p_{3/2}$.

These results are modified here for the states $1s^2\,nlj$ of the non-H atoms (ions). It is supposed that for any ion with *nlj* electron over the core of closed shells the sought value may be presented in the form [52]:

$$E_{SE}\left(Z,nlj\right)=0.027148\,\frac{\xi^4}{n^3}\,f\left(\xi,nlj\right)\left(cm^{-1}\right) \qquad (20)$$

The parameter $\xi=(E_R)^{1/4}$, E_R is the relativistic part of the bounding energy of the outer electron; the universal function $f(\xi,nlj)$ does not depend on the composition of the closed shells and the actual potential of the nucleus.

The procedure of generalization for a case of the non-H systems with the finite nucleus consists of the following steps [9,]:

1). Calculation of the values E_R and ξ for the states *nlj* of H-like ions with the point nucleus (in accordance with the Zommerfeld formula);

2). Construction of an approximating function $f(\xi,nlj)$ by the found reference *Z* and the appropriate $F(H|Z,nlj)$; 3). Calculation of E_R and ξ for the states *nlj* of *Li*-like ions with the finite nucleus; 4). Calculation of E_{SE} for the sought states

by the formula (14). The energies of the states of the non-H atoms and ions are calculated twice: with a conventional constant of the fine structure $\alpha = 1/137$ and with $\tilde{\alpha} = \alpha/1000$.

The results of latter calculations were considered as non-relativistic. This permitted isolation of E_R and ξ.

A detailed evaluation of their accuracy may be made only after a complete calculation of $E^n_{SE}(Z,nlj)$.

It may be stated that the above extrapolation method is more justified than using the widely spread expansions by the parameter αZ. The other details of the theory and computational code can be found in Refs.[61-70, 76-79].

2.4 Elements of Relativistic energy approach

Let us remind that an initial general energy formalism combined with an empirical model potential method in a theory of atoms and multicharged ions has been developed by Ivanov-Ivanova et al [80-84]; further more general ab initio gauge-invariant version of relativistic energy approach has been presented by Glushkov-Ivanov [89]. The imaginary part of the energy shift of an atom is connected with the radiation decay possibility (transition probability). For the α-n radiation transition ImΔE in the lowest order of the PT is determined as:

$$\mathrm{Im}\,\Delta E = -\frac{1}{4\pi}\sum_{\substack{\alpha>n>f \\ [\alpha<n\le f]}} V^{|\omega_{\alpha n}|}_{\alpha n \alpha n}, \tag{21a}$$

where $\omega_{\alpha n}$ is a frequency of the α-n radiation, (α>n>f) for particle and (α<n<f) for vacancy. The matrix element V is determined as follows:

$$V^{|\omega|}_{ijkl} = \iint dr_1 dr_2 \Psi^*_i(r_1)\Psi^*_j(r_2)\frac{\sin|\omega|r_{12}}{r_{12}}(1-\alpha_1\alpha_2)\Psi^*_k(r_2)\Psi^*_l(r_1) \tag{21b}$$

The detailed procedure for computing the matrix elements (22) is presented in Refs. [76-88]. All calculations are performed with using the numeral code Superatom (version 98).

The imaginary part Q^{Cul}_λ contains the radial R_λ and angular S_λ integrals as follows:

$$\mathrm{Im}\,Q_\lambda^{Cul}(12;43) = Z^{-1}\,\mathrm{Im}\{R_\lambda(12;43)S_\lambda(12;43) + R_\lambda(\tilde{1}2;4\tilde{3})S_\lambda(\tilde{1}2;4\tilde{3}) +$$

$$+R_\lambda(1\tilde{2};\tilde{4}3)S_\lambda(1\tilde{2};\tilde{4}3) + R_\lambda(\tilde{1}\tilde{2};\tilde{4}\tilde{3})S_\lambda(\tilde{1}\tilde{2};\tilde{4}\tilde{3})\}. \qquad (21c)$$

In the non-relativistic limit there remains only the first term in (44) depending only on the large component $f(r)$ of the one-electron Dirac functions:

$$\mathrm{Im}\,R_\lambda(12;43) = \frac{1}{2}(2\lambda+1)\pi X_\lambda(13)X_\lambda(24)$$

$$X_\lambda(12) = \int dr\, r^{3/2}\, f_1(r) J^{(1)}_{\lambda+1/2}\left(r\alpha Z|\omega| f_2(r)\right) \qquad (21d)$$

The angular coefficient has only a real part:

$$S_\lambda(12;43) = S_\lambda(13)S_\lambda(24)$$

$$S_\lambda(13) = \{\lambda l_1 l_3\}\begin{pmatrix} j_1 & j_3 & \lambda \\ \frac{1}{2} & -\frac{1}{2} & 0 \end{pmatrix} \qquad (21e)$$

$\{\lambda l_1 l_3\}$ means that λ, l_1 and l_3 must satisfy the triangle rule and the sum $\lambda + l_1 + l_3$ must be an even number.

The rest terms in (44) include the small components of the Dirac functions. The tilde designates that the large radial component f must be replaced by the small one g, and instead of $l_i, \tilde{l}_i = l_i - 1$ should be taken for $j_i < l_i$ and $\tilde{l}_i = l_i + 1$ for $j_i > l_i$.

Only the phase factor of the formulae (43)-(45) depends on the orbital momenta l_i.

Such a simple form of the angular part of the matrix elements has been derived by Kanjauskas and Rudzikas (1975; see Refs. [3,4,90-94]) when calculating $\mathrm{Re}\,\Delta E$.

The problem of the searching for the optimal one-electron representation is one of the oldest in the theory of multielectron atoms. Two decades ago Davidson had pointed the principal disadvantages of the traditional representa-

tion based on the self-consistent field approach and suggested the optimal "natural orbitals" representation. Nevertheless there remain insurmountable calculational difficulties in the realization of the Davidson program.

One of the simplified recipes represents, for example, the DFT method [29-33]. Unfortunately, this method doesn't provide a regular refinement procedure in the case of the complicated atom with few quasiparticles (electrons or vacancies besides the core of closed shells).

In the theory of radiative and nonradiative decay of the quasistationary states of a multielectron atom it is well known an energy approach (see below) , based on the adiabatic Gell-Mann and Low formula [89,117,128] for the energy shift δE with electrodynamic scattering matrice. The method is a consistently electrodynamic one, allowing for the uniform consideration of a variety of induced and spontaneous processes different by their physical nature [129-156].

For simplicity, let us consider now the one-quasiparticle system. The multiquaiparticle case doesn’t contain principally new moments. In the lowest, second order, of the QED PT for the δE there is the only one- quasiparticle Feynman diagram A (fig.1), contributing the Im δE (the radiation decay width).

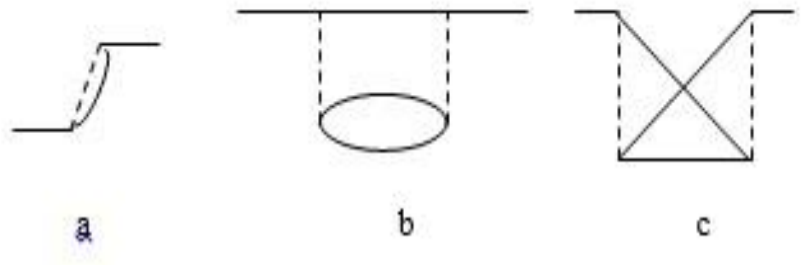

Figure 1 – a: second other EDPT diagram contributing the imaginary energy part related to the radiation transitions. b and c: fourth order polarization diagrams

Our density functional method, based on the formally exact QED PT, uses for this purpose the model bare potential, constructed with accounting for the spectroscopic information concerning simplest systems with one quasiparticle [90].

In the next, the fourth order there appear diagrams, whose contribution into the ImδE account for the core polarization effects. This contribution describes collective effects and it is dependent upon the electromagnetic poten-

tials gauge (the gauge noninvariant contribution). Let us examine the multielectron atom with one quasiparticle in the first excited state, connected with the ground state by the radiation transition. In the zero QED PT approximation we, as usually (see ref.[128]), use the one electron bare potential:

$$V_N(r)+V_C(r), \tag{22a}$$

with $V_N(r)$ describing the electric potential of the nucleus, $V_C(r)$, imitating the interaction of the quasiparticle (initial or any other appearing in the real and virtual processes) with the core of closed shells. The perturbation in terms of the second quantization representation reads

$$-V_C(r)\ \psi^+(r)\ \psi(r)\ -\ j_\mu(x)\ A^\mu(x) \tag{22b}$$

The core potential $V_C(r)$ is related to the core electron density $\rho_C(r)$ in a standard way. The latter fully defines the one electron representation. Moreover, all the results of the approximate calculations are the functionals of the density $\rho_C(r)$. Here, the lowest order multielectron effects, in particular, the gauge dependent radiative contribution for the certain class of the photon propagator calibration is treating.

This value is considered to be the typical representative of the electron correlation effects, whose minimization is a reasonable criteria in the searching for the optimal one-electron basis of the PT. Besides, this procedure derives an undoubted profit in the routine spectroscopic calculations as it provides the way of the refinement of the atomic characteristics calculations, based on the "first principles" .

Remember that the closeness of the radiation probabilities calculated with the alternative forms of the transition operator is commonly used as a criterion of the multielectron calculations quality. It is of special interest to verify the compatibility of the new optimization principle with the other requirements conditioning a "good" one-electron representation.

The imaginary part of the diagram a (fig.1) contribution in the case of the Lorentz calibration has been presented previously as a sum of the partial contributions of α-s transitions from the initial state α to the final state s [3,128],

$$\mathrm{Im}\delta E_\alpha\,(\mathrm{a}) = \sum_s \quad \mathrm{Im}\ \delta E\ (\alpha\text{-}s;\ \mathrm{a}). \qquad (22c)$$

Two fourth order polarization diagrams b,c (fig.1) are considered in this article. The contributions being under consideration, are gauge- dependent, though the results of the exact calculation of any physical quantity must be gauge independent . All the noninvariant terms are multielectron by their nature. Let us take the photon propagator calibration as follows:

$$D = D_{\mathrm{T}} + CD_{\mathrm{L}},$$

$$D_{\mathrm{T}} = \delta_{\mu\nu} / (k_0^2 - k^2),$$

$$D_{\mathrm{L}} = - k_\mu k_\nu / (k_0^2 - k^2). \qquad (23)$$

Here, D_{T} represents the exchange of electrons by transverse photons, D_{L} that by longitudinal ones. The values C=0 and C=1 of the gauge constant are related to the Lorentz and to the Landau calibrations correspondingly. One could calculate the contribution of the a,b,c diagrams (fig.1.1) into the Im δE taking into account both the D_{T} and D_{L} parts.

The A diagram contribution into the Im δE related to the α -s transition reads as

$$-\frac{e^2}{8\pi}\int\int \mathrm{d}r_1\mathrm{d}r_2\,\psi_\alpha^+(r_1)\ \psi_s^+(r_2)\ \frac{1-\alpha_1\alpha_2}{r_{12}}\sin(\omega_{\alpha s} r_{12})\ \psi_\alpha(r_2)\ \psi_s(r_1), \qquad (24)$$

for $D = D_{\mathrm{T}}$, and

$$-\frac{e^2}{8\pi}\int\int \mathrm{d}r_1\,\mathrm{d}r_2\ \psi_\alpha^+(r_1)\ \psi_s^+(r_2)\ \{[(1-\alpha_1 n_{12}\,\alpha_2 n_{12})/ r_{12}]\sin(\omega_{\alpha s} r_{12}) +$$
$$+\omega_{\alpha s}\,(1+\alpha_1 n_{12}\alpha_2 n_{12})\times\cos(\omega_{\alpha s} r_{12})\}\,\psi_\alpha(r_2)\,\psi_s(r_1), \qquad (25)$$

for D=D_{L}, where $\omega_{\alpha s}$ is the α -s transition energy.

According to the Grant theorem [1], the $D_{\mu\nu,\mathrm{L}}$ contribution vanishes, if the one-quasiparticle functions ψ_α , ψ_s satisfy the same Dirac equation. Nevertheless this term is to be retained when using the distorted waves approximation, for example.

Another very important example represents the formally exact approach based on the bare hamiltonian defined by its spectrum without specifying its analytic form [129,130]. Here the noninvariant contribution appears already in the lowest order. When calculating the forth order contributions some approximations are inevitable. These approximations have been formulated in Refs.[90, 94,96], where the polarization corrections to the state energies have been considered. Here, we reproduce briefly the calculational scheme.

Let us consider the direct polarization diagram as an example. After the linearization over the gauge constant *C*, the formal expression for the sought for value looks as

$$Im\delta E_{ninv}(\alpha - s \mid b) = -C\frac{e^2}{4\pi}\int\int\int\int dr_1 dr_2 dr_3 dr_4 \sum_{n>f,\, m\le f} \left(\frac{1}{\omega_{mn}+\omega_{\alpha s}} + \frac{1}{\omega_{mn}-\omega_{\alpha s}}\right) \times$$

$$\times \Psi^+_\alpha(r_1)\Psi^+_m(r_2)\Psi^+_s(r_4)\Psi^+_n(r_3)\cdot[(1-\alpha_1\alpha_2)/r_{12}]\cdot\{[\alpha_3\alpha_4-(\alpha_3 n_{34})(\alpha_4 n_{34})]/r_{34}$$

$$\times \sin[\omega_{\alpha n}(r_{12}+r_{34})]+[1+(\alpha_3 n_{34})(\alpha_4 n_{34})]\omega_{\alpha n}\cos[\omega_{\alpha n}(r_{12}+r_{34})]\}$$

$$\times \Psi_m(r_3)\Psi_\alpha(r_4)\Psi_n(r_2)\Psi_s(r_1). \qquad (26)$$

and the upper continuum electron states; $m \le f$ indicates the finite number of states in the core and the states of the negative continuum (accounting for the electron vacuum polarization).

All the vacuum polarization and the self-energy corrections to the sought for values are omitted. Their numerical smallness compared with the other relativistic corrections to the different atomic characteristics had been verified by the numerous calculations. The renormalization procedure is not needed here. Nevertheless the second-order vacuum polarization and self-energy corrections can be additively added to the complex state energy. The remaining expression includes summation over the bound and upper continuum atomic states.

To evaluate this sum, we use the analytic relation between the atomic electron Fermi level and the core electron density $\rho_c(r)$, appropriate to the homogeneous nonrelativistic electron gas (the Tomas- Fermi approximation). Now the sum $\sum_{n>f,\, m<f}$ can be calculated analytically , its value becomes a functional of the core electron density. The resulting expression looks as the

correction due to the additional nonlocal interaction of the active quasiparticle with the closed shells.

Nevertheless its calculation is reducible to the solving of the system of the ordinary differential equations - the one- dimensional procedure. The most important refinements can be introduced by accounting for the relativistic and the density gradient corrections to the Tomas- Fermi formula (see Refs. [3,4]). The same program is realized for the remaining forth order QED PT polarization corrections.

The minimization of the functional Im δE_{ninv} (b+c) leads to the integro- differential equation for the ρ_{c} (the Dirac-Fock or Dirac-Kohn-Sham-like equations for the electron density) that can be solved using one of the standard numerical codes.

As a result one can get the optimal PT one-quasi-particle basis.

In concrete calculations it is sufficient to use a more simplified procedure, which is reduced to the functional minimization using the variation of the correlation potential parameter *b* in Eq. (13) or (17) [3,4,117,128].

2.5 Some Results and Conclusions

Below we present some results of calculation of the energy and spectroscopic characteristics for kaonic atoms of the hydrogen and nitrogen. The kaonic hydrogen atom is of a considerable interest as a meson atom that has no electron subsystem.

The results of experimental study of the hydrogen KA has been presented, for example, in Refs. [3,4]. In particular, the X-ray 2-1 transition in the kaon H spectrum is studied obtained in experiment by SIDDHARTA Collaboration (see details in Refs. [3,4]).

In Table 1 there are presented the results of calculating the binding energy of different atomic levels in a hydrogen KA (in keV) obtained in the H-like model of Iwasaki, the method by Indelicato et al and our approach. The Fermi model of a charge distribution in a nucleus is used in our computing [53-56]. In principle, all approaches naturally give fairly close results. Note that the contribution of radiation corrections here is extremely small, in contrast to KA with a large value of the nuclear charge.

Table 1 – Calculated binding energies of different atomic levels in hydrogen KA (in keV)

Level	Indelicato et al	Iwasaki	Our data
1s	8.63360	8.634	8.63380
2p	2.15400	2.154	2.15390
3p	0.95720	0.957	0.95710

In Table 2 there are presented the experimental and theoretical values of the energy (keV) of the 2-1 transition to the hydrogen KA [1-4,7,43,44,53-56]. Experimental data ware listed in Refs. [3,4]. Theoretical results are obtained on the basis of calculations within the method by Indelicato et al [42,43] and our relativistic approach.

Table 2 - The experimental E_{exp} and theoretical E_c values of energy (keV) of the 2-1 transition in the hydrogen KA spectrum (see text)

E_c, This work	E_c [44,50]	E_{exp} [1-4]
6.481	6.480 6.482	6,44±0,4 6.675±0,15 6,96±0,33

As in the case of the energies of atomic levels, there is a fairly good agreement between the theoretical results (in fact, the electromagnetic contributions to the transition energy!), which is explained by the insignificant role of radiative corrections (in the absence of electrons). We have performed the calculation of the transition energy using charge distribution models in the form of a uniformly charged ball, the Gauss distribution and the Fermi model. The difference in the corresponding values of energies averaged a few eV (compared to keV), thus, in this case, the choice of the charge distribution model is not critical. On the other hand, for radiative transitions between low-lying energy levels (n ~ 1), as in our case, the contribution due to the strong interaction is very significant. The strong kaon-nucleon interaction induces a shift and broadening of the 1s level in the spectrum of kaonic hydrogen. The corresponding shift in the pres-

ence of an experimental value of the transition energy, say, $E_{exp}(2p\text{-}1s)$ and a "precisely" defined "electromagnetic" correction E^{EM} is defined as:

$$\Delta E(1s)= E_{exp}(2p\text{-}1s)- E^{EM}(2p\text{-}1s).$$

According to the experimental data by M. Iwasaki et al (KEK, 1997), as well as T. Ito, R. Hayano, S. Nakamura et al (2007), the measured shift is as follows:

$$\Delta E_{1s}=-323\pm63(stat.)\pm11(syst.)\ eV$$

It is appropriate to present the results of earlier experiments (see, for example, [41]), in particular, according to the measurements by Davies et al (1979):

$$\Delta E_{1s}=+40\text{-}50\ eV,\ Bird\ et\ al\ (1983)$$

$$\Delta E_{1s}=+180\text{-}190\ ,\ Izycki\ et\ al\ (1980)$$

$$\Delta E_{1s}=+260\text{-}270\ eV.$$

Finally, the most recent DEAR (DAFNE Exotic Atom Research) experiment, performed on the DAFNE facility at the Frascatti laboratory (Frascatti, Italy, 2005), allowed to get the following result:

$$\Delta E_{1s}=-194\pm37(stat.)\pm6(syst.)\ eV;$$

Now using the “electromagnetic” values of the transition energy, obtained in theoretical calculation and the latest experimental values available, it is not difficult to estimate the shift of the 1s level in spectrum of the kaonic hydrogen due to the strong kaon-nucleon interaction. For different values $E_{exp}(2p\text{-}1s)$ then one could obtain:

$$\Delta E_{1s}=-6440+6481=41эВ,\ \Delta E_{1s}=-6675+6481=-194\ eV,$$

$$\Delta E_{1s}=-6960+6481=-479\ eV.$$

Note that the exact coincidence of the theoretically estimated (-194 eV) and the experimental and measured "strong" shift here is, obviously, fortunately

random. In contrast to the considered below kaonic helium, the "strong" shift of the 1s level in the hydrogen atom is rather large in absolute value.

In any case, the calculated "electromagnetic" value of the transition energy and further comparison with the experimental value of the transition allowed us to obtain a theoretical estimate of the "strong" shift in kaonic hydrogen, which is in excellent agreement with the DEAR experimental shift.

Spectrum of kaonic nitrogen. Hyperfine structure and radiative transitions probabilities

The kaonic nitrogen atom (^{14}N), like the previous case of the kaonic hydrogen, belongs to the light KA. Its study is of a great interest, first of all, from the point of view of developing new X-ray standards. As a model of the charge distribution in the nucleus, we applied the model of a uniformly charged ball, the Gauss model, and the Fermi model. The influence of the choice of the potential describing the effect of vacuum polarization on the energy parameters of KA has been in details studied too.

To take into account the effect of vacuum polarization, we used the standard Uehling-Serber potential and the generalized potential of the form [1] taking into account the finite size of KA nucleus. The relativistic QED corrections of higher orders are also taken into account, including the relativistic recoil correction.

In Table 3 there are presented the results of calculating the energy (electromagnetic) contributions (the main Coulomb correction, the correction for the vacuum polarization, the relativistic correction for the recoil effect and the hyperfine shift) to the 8k-7i transition energy in the spectrum of kaonic nitrogen: the data of calculations on the basis of theory by Indelicato et al [43,50] and our theoretical approach.

Table 3 also shows the error caused by the inaccuracy in determining the mass of the K^-kaon. Our values, given in Table 3, correspond to the Gaussian model of charge distribution in the nitrogen nucleus.

Calculation using other models showed the difference, which is for the model of a uniformly charged ball (0.8 eV) and the Fermi model (0.5 eV).

Table 3 – Energy contributions (in eV) to the 8k-7i transition energy in the spectrum of kaonic nitrogen

Contributions	8k-7i, Theory [43,50]	8k-7i Present work
Coulomb Contribution	2968.4565	2968.4492
Vacuum polarization	1.1789	1.1778
Relativistic recoil effect	0.0025	0.0025
Hyperfine shift	-0.0006	-0.0007
Full energy	2969.6373	2969.6288
Error	0.096	0.096

The value corresponding to the correction for vacuum polarization, obtained in the approximation of the standard Uehling-Serber potential (i.e., without taking into account the contribution of the vacuum of polarization corrections of higher orders in the parameter $z\alpha$, namely Wichmann-Kroll, Calen-Sabri, etc.) is 1.1665 eV, while the corresponding value with accounting for the indicated corrections is 1.1778 eV.

According to estimates by Indelicato et al. [43, 50], who performed a complete calculation of the vacuum of polarization corrections of higher orders in the parameter, the sought contribution is 0.01 eV.

Thus, the use of the generalized Uehling-Serber potential turns out to be more efficient in comparison with the standard Uehling-Serber approximation, which is usually used in calculating the spectra of both usual (purely multielectron) and exotic atomic systems.

On the other hand, for atoms with a low nuclear charge, the sought contribution to the vacuum of polarization corrections remains insignificant. Naturally, with an increase in the nuclear charge, in the transition to heavy KA, this contribution will increase significantly.

The PT formalism for evaluating the vacuum of polarization corrections of higher orders in terms of $z\alpha$, naturally, ceases to be correct, and a nonperturbative approach is required here.

In Table 4 we present the results of calculating the energies (in eV) of transitions between the components of the hyperfine structure 8k-7i in a spectrum of

the kaonic nitrogen: 1) the theoretical data, obtained within the theory by Inelicato et al [43,50] and our theoretical approach.

Table 4 – Energies (in eV) of transitions between the components of the hyperfine structure 8k-7i in the spectrum of kaonic nitrogen

F-F’	ΔE, Theory [43,50]	ΔE, Present work
8-7	2969.6365	2969.6289
7-6	2969.6383	2969.6298
7-7	2969.6347	2969.6264
6-5	2969.6398	2969.6345
6-6	2969.6367	2969.6284
6-7	2969.6332	2969.6248

Similarly, in Table 5 we present the results of calculating a probabilities A (in 10^{13} s^{-1}) of the transitions between the components of the hyperfine structure 8k-7i in the spectrum of kaonic nitrogen: 1) the theoretical data , obtained on the basis of calculation within the theory by Indelicato et al [43,50] and 2) data, obtained on the basis of our theoretical approach.

Analysis of the data presented shows, in principle, a reasonable agreement between the results of both theories. It should be noted that the radiative corrections are taken into account in our theory within the combined generalized Uehling-Serber approach and method [2].

This, on the one hand, explains the difference in the results, on the other hand, the data we obtained should be considered as the most accurate at the moment. The same applies to the analysis of the obtained values of the probabilities of transitions between the components of the hyperfine structure 8k-7i in the spectrum of kaonic nitrogen.

The considered transitions in the spectrum of kaonic nitrogen actually belong to the so-called Rydberg transitions, which largely demonstrate hydrogen-like properties; therefore, as a rule, the results of various theories for such transitions are, as a rule, in good agreement with each other.

Table 5 – Probabilities A (10^{13} c^{-1}) of transitions between the components of the hyperfine structure 8k-7i in the spectrum of kaonic nitrogen

F-F’	A Theory [43,50]	A This work
8-7	1.54×10^{13}	1.51×10^{13}
7-6	1.33×10^{13}	1.32×10^{13}
7-7	1.31×10^{13}	1.29×10^{13}
6-5	1.15×10^{13}	1.12×10^{13}
6-6	0.03×10^{13}	0.02×10^{13}
6-7	-	0.004×10^{13}

In Table 6 we present the results of our calculation of the energy (electromagnetic) contributions (the main Coulomb correction, the correction for vacuum polarization, the relativistic correction for the recoil effect and the hyperfine shift) to the 8i-7h transition energy in the spectrum of kaonic nitrogen.

Table 6 – Energy contributions (in eV) to the 8i-7h transition energy in the spectrum of kaonic N

Contributions	8i-7h Present work
Coulomb Contribution	2968.5344
Vacuum polarization	1.8758
Relativistic recoil	0.0025
Hyperfine shift	-0.0009
Full energy	2970.4118
Error	0.096

The data on the energy contributions presented here correspond to the use of the Gaussian model of the charge distribution in the nucleus.

Similarly to the previous case, an error is also indicated due to the in accuracy in determining the mass of the K^-. kaon.

The value corresponding to the correction for the polarization of the core, obtained in the generalized Uehling-Serber approximation (i.e., taking into account the contribution of the vacuum of polarization corrections of higher orders in the parameter $Z\alpha$) is 1.8758 eV.

Further, in Table 8 we present the results of our calculation of the energies (in eV) of transitions between the components of the hyperfine structure 8i-7h in the spectrum of kaonic nitrogen.

Table 7 – Energies (in eV) of transitions between the components of the hyperfine structure 8i-7h in the spectrum of kaonic nitrogen

F-F’	ΔE, This work
7-6	2970.4107
6-5	2970.4135
6-6	2970.4086
5-4	2970.4193
5-5	2970.4114
5-6	2970.4073

Correspondingly, in Tables 8 and 9 we present the results of our calculation of probabilities A (in 10^{13} s^{-1}) of transitions between the hyperfine structure components 8i-7h and 7h-6g in the spectrum of kaonic nitrogen. Note that, for the first time in a theory of the kaonic atomic systems, a consistent relativistic energy approach has been generalized and applied to calculating the probabilities of radiative transitions between the components of the hyperfine structure,

Table 8 – Probabilities A (10^{13}, s^{-1}) of transitions between components of the hyperfine structure 8i-7h in the spectrum of kaonic nitrogen

F-F’	P, This work
7-6	1.16×10^{13}
6-5	0.99×10^{13}
6-6	0.96×10^{13}
5-4	0.81×10^{13}
5-5	0.02×10^{13}
5-6	0.005×10^{13}

Table 9 – Probabilities A (10^{13}, s^{-1}) of transitions between the components of the hyperfine structure 7h-6g in the spectrum of kaonic nitrogen

F-F’	P, This work
6-5	0.82×10^{13}
6-6	0.76×10^{13}
5-4	0.42×10^{13}
5-5	0.01×10^{13}
5-6	0.001×10^{13}

To conclude, let us note that a consistent relativistic approach to calculation of energy and spectral parameters of the kaonic exotic atomic systems with accounting for the nuclear radiative (quantum electrodynamics), hyperfine and strong interactions is presented.

The approach is naturally based on using the relativistic Klein-Gordon-Fock equation with introduction of electromagnetic and strong interactions potentials. To take a strong kaon-nuclear interaction into account, the generalized optical potential method is applied. As an illustration, different results of computing the energy and spectral characteristics for some kaonic atoms are presented.

In particular, the results of calculating the binding energies of various atomic levels in the hydrogen and nitrogen kaonic atoms are listed and obtained within the H-like model of Iwasaki, the method of Indelicato et al and our approach (here the Fermi model of the charge distribution in the nucleus is used). In addition, the results of calculating the energy (electromagnetic) contributions (the main Coulomb correction, correction for vacuum polarization, relativistic correction for the recoil effect, a hyperfine shift) to the energy of the 8k-7i, 8i-7h transitions in the spectrum of kaonic nitrogen are listed too.

In principle, one should keep in mind that a physically reasonable agreement between experimental and theoretical data for the kaonic atomic systems can be achieved only with simultaneous accurate and correct consideration of relativistic, radiation, and nuclear effects. The further improvement and refinement of the theoretical approach and increasing the calculational data accuracy should include the corresponding development of model of the strong kaon-nuclear interaction such as receiving more exact data about the kaon-nuclear potential parameters.

CONCLUSIONS

We present a consistent relativistic approach to calculation of energy and spectral parameters of the kaonic exotic atomic systems with accounting for the nuclear radiative (quantum electrodynamics), hyperfine and strong interactions. The approach is naturally based on using the relativistic Klein-Gordon-Fock equation with introduction of electromagnetic and strong interactions potentials. To take a strong kaon-nuclear interaction into account, the generalized optical potential method is applied. In order to take the nuclear (the finite nuclear size effect) and radiative (quantum electrodynamics) corrections into account, the generalized Uehling-Serber approach is applied. The elements of the hyperfine structure theory of the kaonic atoms (KA) are presented. As an illustration, there are results of calculating the binding energies of various atomic levels in a hydrogen KA obtained within the H-like model of Iwasaki, the method of Indelicato et al and our approach (here the Fermi model of the charge distribution in the nucleus is used). Using our calculated "electromagnetic" values of the transition energy and a set of available latest experimental values, it is calculated a shift of the 1s level in kaonic hydrogen, due to the strong kaon-nucleon interaction; the calculated "electromagnetic" value of the transition energy and further comparison with the experimental value of the transition allowed to obtain a theoretical estimate of the "strong" shift in kaonic hydrogen, which is in excellent agreement with the DEAR experimental data. In addition, the results of calculating the energy (electromagnetic) contributions (the main Coulomb correction, correction for vacuum polarization, relativistic correction for the recoil effect, a hyperfine shift) to the energy of the 8k-7i, 8i-7h transitions in the spectrum of kaonic nitrogen are presented and compared with the alternative theoretical data by Indelicato et al.

REFERENCES

1. Grojean C (2007) New approaches to electroweak symmetry breaking. Physics-Uspekhi 50:3-42.
2. Khetselius OYu (2011) Quantum structure of electroweak interaction in heavy finite Fermi-systems. Astroprint, Odessa.
3. Glushkov A, Khetselius O, Lovett L (2009) Electron-β-nuclear spectroscopy of atoms and molecules and chemical bond effect on the β-decay parameters. In: Piecuch P, Maruani J, Delgado-Barrio G, Wilson S (eds) Advances in the Theory of Atomic and Molecular Systems Dynamics, Spectroscopy, Clusters, and Nanostructures. Series: Progress in Theor. Chem. and Phys., vol 20. Springer, Dordrecht, pp 125-152.
4. Dzhelepov BS, Zyryanova LP and Suslov YP (1978) Beta processes. Functions for the analysis of beta spectra and electron capture. Nauka, Leningrad.
5. Harston MR, Pyper NC (1986) On estimates of probabilities for beta decay of a Nucleus with capture on electron shells. Phys. Rev. Lett. 56:1790-1795.
6. Haxton WC, Liu CP, Ramsey-Musolf MJ (2001) Anapole Moment and Other Constraints on the Strangeness Conserving Hadronic Weak Interaction. Phys.Rev.Lett. 86:5247-5250.
7. Haxton WC, Liu CP, Ramsey-Musolf MJ (2002) Nuclear anapole moments. Phys. Rev. C. 65:045502.
8. Izosimov IN, Kazimov AA, Kalinnikov VG, Solnyshkin AA, Suhonen J (2004) Beta-Decay Strength Measurement, Total Beta-Decay Energy Determination and Decay-Scheme Completeness Testing by Total Absorption gamma-ray Spectroscopy. Phys. Atom. Nucl. 67(10):1876-1882.
9. Tegen R (2002) Beta decay of the free neutron and a (near) degenerate neutrino mass. Nucl. Phys. A 706:193-202.
10. Glushkov AV (2008) Relativistic Quantum Theory. Quantum, mechanics of atomic Systems. Astroprint, Odessa.
11. Khetselius OYu (2008) Hyperfine structure of atomic spectra. Astroprint, Odessa.
12. Band IM, Listengarten MA and Trzhaskovskaya MV (1986) Calculation of hyperfine structure constants of spectra of heavy ions based on the Hartree-Fock-Dirac method. Izv. AN USSR. 50:2240-2244.
13. Band IM, Listengarten MA and Trzhaskovskaya MV (1986) Probability of β-decay in the Hartree-Fock-Dirac model of the atom and the influence of the chemical environment on β-decay. Izv. AN USSR. Ser. Phys. 51:1998-2004.

14. Bandurina LA, Lendel AI, Medvedev SY (1987) Processes in the electron shell accompanying β-decay of nickel and determination of the boundary energy of the β-spectrum. Nucl. Phys. 45:.642-646.
15. Auerbach N (2008) Search for electric dipole moments in atoms of radioactive nuclei. J Phys G: Nucl Part Phys 35:P014040.
16. Serot BD, Walecka JD (1986) Advances in Nuclear Physics. The Relativistic Nuclear Many Body Problem, vol 16. Plenum Press, New York.
17. Turin AV, Khetselius OY, Dubrovskaya YV (2007) The beta electron final state interaction effect on beta decay probabilities for ^{42}Se nucleus within relativistic Hartree-Fock approach. Photoelectronics. 16:120-122.
18. Malinovskaya SV, Dubrovskaya YuV, Vitavetskaya LA (2005) Advanced Quantum Mechanical Calculation of the Beta Decay Probabilities. Energy approach to resonance states of compound superheavy nucleus and EPPP in heavy nuclei collisions. In: Grzonka D., Czyzykiewicz R., Oelert W., Rozek T., Winter P. (eds) Low Energy Antiproton Physics. AIP: New York, AIP Conf. Proc. 796:201-205.
19. Malinovskaya SV, Dubrovskaya YuV, Zelentzova TN 92004) The atomic chemical environment effect on the β decay probabilities: Relativistic calculation. Herald of Kiev Nat Univ. Series: Phys Math 4:427-432.
20. Malinovskaya SV, Glushkov AV, Dubrovskaya YV, Vitavetskaya LA (2006) Quantum calculation of cooperative muon-nuclear processes: Discharge of metastable nuclei during negative muon capture. In: Julien J-P, Maruani J, Mayou D, Wilson S, Delgado-Barion G (eds) Recent Advances in the Theory of Chemical and Physical Systems. Series: Progress in Theoretical Chemistry and Physics, vol 15. Springer, Dordrecht, pp 301-306.
21. Khetselius OYu, Lopatkin YuM, Dubrovskaya YuV, Svinarenko AA (2010) Sensing hyperfine-structure, electroweak interaction and parity non-conservation effect in heavy atoms and nuclei: New nuclear-QED approach. Sensor Electr and Microsyst. Techn. 7(2):11-19.
22. Kopytin IV, Karelin KN, Nekipelov AA (2004) Exact Inclusion of the Coulomb Field in the Photobeta Decay of a Nucleus and Problem of Bypassed Elements. Phys. Atom. Nucl. 67(8):1429-1441.
23. Khetselius OYu, Glushkov AV, Dubrovskaya YuV, Chernyakova YuG, Ignatenko AV, Serga IN, Vitavetskaya LA (2018) Relativistic quantum chemistry and spectroscopy of exotic atomic systems with accounting for strong interaction effects. In: Wang YA, Thachuk M, Krems R, Maruani J (eds) Concepts, Methods and Applications of Quantum Systems in Chemistry and

Physics. Series: Progress in Theoretical Chemistry and Physics, vol 31. Springer, Cham, pp 71-91.
24. Glushkov AV, Lovett L, Khetselius OYu, Gurnitskaya EP, Dubrovskaya YuV, Loboda AV (2009) Generalized multiconfiguration model of decay of multipole giant resonances applied to analysis of reaction (μ-n) on the nucleus ^{40}Ca. Int. Journ. of Modern Phys. A 24(2-3):611-615.
25. Glushkov AV, Rusov VD, Ambrosov SV, Loboda AV (2003) Resonance states of compound super-heavy nucleus and EPPP in heavy nucleus collisions. In: Fazio G, Hanappe F (eds) New Projects and New Lines of Research in Nuclear Physics. World Scientific, Singapore, pp126-132.
26. Glushkov AV, Ambrosov SV, Khetselius OYu et al (2004) QED calculation of the super heavy elements ions: energy levels, radiative corrections and hfs for different nuclear models. Nucl Phys A: Nucl and Hadr Phys 734:21-28.
27. Glushkov AV, Ambrosov SV, Loboda AV, Gurnitskaya EP, Khetselius OY (2005) QED calculation of heavy multicharged ions with account for correlation, radiative and nuclear effects. In: Julien J-P, Maruani J, Mayou D, Wilson S, Delgado-Barion G (eds) Recent Advances in Theor. Phys. and Chem. Systems. Series: Progress in Theoretical Chemistry and Physics, vol 15. Springer, Dordrecht, pp 285-299.
28. Glushkov AV, Gurskaya M Yu, Ignatenko AV, Smirnov AV, Serga IN, Svinarenko AA, Ternovsky EV (2017) Computational code in atomic and nuclear quantum optics: Advanced computing multiphoton resonance parameters for atoms in a strong laser field. J. Phys: Conf. Ser. 905(1): 012004.
29. Dubrovskaya YuV, Khetselius OYu, Vitavetskaya LA, Ternovsky VB, Serga IN (2019) Quantum Chemistry and Spectroscopy of Pionic Atomic Systems with Accounting for Relativistic, Radiative, and Strong Interaction Effects. Adv Quantum Chem. Elsevier 78:193-222. https://doi.org/10.1016/bs.aiq.2018.06.003.
30. Ivanova EP, Ivanov LN, Glushkov AV and Kramida AE (1985) High Order Corrections in the Relativistic Perturbation Theory with the Model Zeroth Approximation, Mg-Like and Ne-Like Ions. Phys.Scripta. 32(5):513-522.
31. Khetselius O Yu, Glushkov AV, Gurskaya MYu, Kuznetsova AA, Dubrovskaya YuV, Serga IN and Vitavetskaya LA (2017) Computational modelling parity nonconservation and electroweak interaction effects in heavy atomic systems within the nuclear-relativistic many-body perturbation theory. J. Phys.: Conf. Ser. 905:012029.

32. Khetselius OY (2007) Hyperfine structure of energy levels for isotopes 73Ge, 75As, 201Hg. Photoelectronics 16:129-132.
33. Khetselius OYu (2008) On possibility of sensing nuclei of the rare isotopes by means of laser spectroscopy of hyperfine structure. Sensor Electr Microsyst Techn 3:28-33.
34. Khetselius OYu (2008) On sensing nuclei of the lanthanide isotopes by means of laser spectroscopy of hyperfine structure ^{165}Ho, ^{169}Tm. Sensor Electr and Microsyst. Techn. 2:5-9.
35. Khetselius OYu (2009) Atomic parity non-conservation effect in heavy atoms and observing P and PT violation using NMR shift in a laser beam: To precise theory. J Phys: Conf Ser 194:022009.
36. Khetselius OYu (2009) On sensing nuclei of the ^{207}Bi &^{207}Pb isotopes by means of laser spectroscopy of hyperfine. Sensor Electr. and Microsyst. Techn. 2:26-29.
37. Khetselius Oyu (2009) Relativistic calculation of the hyperfine structure parameters for heavy elements and laser detection of the heavy isotopes. Phys Scripta T135:014023.
38. Khetselius OYu (2009) Relativistic perturbation theory calculation of the hyperfine structure parameters for some heavy-element isotopes. Int J of Quantum Chemistry 109:3330-3335.
39. Khetselius OYu (2010) Relativistic hyperfine structure spectral lines and atomic parity nonconservation effect in heavy atomic systems within QED theory. AIP Conf Proc 1290:29-33.
40. Khetselius OYu (2012) Quantum Geometry: New approach to quantization of quasistationary states of Dirac equation for superheavy ion and calculating hyperfine structure parameters. Proc. Intern. Geom. Center 5(3-4):39-45.
41. Khetselius OYu (2012) Relativistic Energy Approach to Cooperative Electron-γ-Nuclear Processes: NEET Effect. In: Nishikawa K, Maruani J, Brändas E, Delgado-Barrio G, Piecuch P (eds) Quantum Systems in Chemistry and Physics: Progress in Methods and Applications. Series: Progress in Theoretical Chemistry and Physics, vol 26. Springer, Dordrecht, pp 217-229.
42. Glushkov AV, Khetselius OY, Dubrovskaya YV, Loboda AV (2006) Sensing the capture of negative muon by atoms: Energy approach. Sensor Electr. and Microsyst. Techn 3:31-35.
43. Glushkov AV, Khetselius OYu, Svinarenko AA (2012) Relativistic theory of cooperative muon-γ -nuclear processes: Negative muon capture and metastable nucleus discharge. In: Hoggan P, Brändas E, Maruani J, Delgado-Barrio

G, Piecuch P (eds) Advances in the Theory of Quantum Systems in Chemistry and Physics. Series: Progress in Theoretical Chemistry and Physics, vol 22. Springer, Dordrecht, pp 51-68.
44. Glushkov AV, Malinovskaya SV, Khetselius OYu, Loboda AV, Sukharev DE, Lovett L (2009) Green's function method in quantum chemistry: New numerical algorithm for the Dirac equation with complex energy and Fermi-model nuclear potential. Int Journ Quant Chem 109:1717-1727.
45. Glushkov AV, Khetselius OYu, Gurnitskaya EP, Loboda AV, Florko TA, Sukharev DE, Lovett L (2008) Gauge-Invariant QED Perturbation Theory Approach to Calculating Nuclear Electric Quadrupole Moments, Hyperfine Structure Constants for Heavy Atoms and Ions. In: Wilson S, Grout PJ, Maruani J, Delgado-Barrio G, Piecuch P (eds) Frontiers in Quantum Systems in Chemistry and Physics. Series: Progress in Theoretical Chemistry and Physics, vol 18. Springer, Dordrecht, pp 507-524.
46. Burvenich TJ, Evers J, Keitel CH (2006) Dynamic nuclear Stark shift in superintense laser fields. Phys. Rev. C. 74:044601.
47. Glushkov AV and Ivanov LN (1993) DC Strong-Field Stark-Effect: consistent quantum-mechanical approach. J.Phys. B: At. Mol. Opt. Phys 26(16):P.L379-L386.
48. Glushkov AV, Ivanov LN (1992) Radiation decay of atomic states: atomic residue polarization and gauge noninvariant contributions. Phys Lett A 170:33-36.
49. Glushkov AV, Ivanov LN., Ivanova EP (1986) Radiation decay of atomic states. Generalized energy approach. In: Autoionization Phenomena in Atoms. Moscow State Univ., Moscow, p 58.
50. Ivanov LN, Ivanova EP, Aglitsky EV (1988) Modern trends in the spectroscopy of multicharged ions. Phys Rep 166:315-388.
51. Ivanova E.P, Glushkov AV (1986) Theoretical investigation of spectra of multicharged ions of F-like and Ne-like isoelectronic sequences. J Quant Spectr Rad Transfer 36 :127-145.
52. Glushkov AV (2006) Relativistic and Correlation Effects in Spectra of Atomic Systems. Astroprint, Odessa.
53. Glushkov AV (2012) Advanced Relativistic Energy Approach to Radiative Decay Processes in Multielectron Atoms and Multicharged Ions. In: Nishikawa K, Maruani J, Brandas E, Delgado-Barrio G, Piecuch P (eds) Quantum Systems in Chemistry and Physics: Progress in Methods and Applications. Series: Progress in Theoretical Chemistry and Physics, vol 26. Springer,

Dordrecht, pp 231-252.
54. Glushkov AV (2012) Spectroscopy of cooperative muon-gamma-nuclear processes: Energy and spectral parameters. J Phys: Conf Ser 397:012011.
55. Glushkov AV (2005) Energy approach to resonance states of compound superheavy nucleus and EPPP in heavy nuclei collisions. In: Grzonka D, Czyzykiewicz R, Oelert W et al (eds) Low Energy Antiproton Physics. AIP Conf Proc, New York, 796:206-210.
56. Glushkov AV (2013) Operator Perturbation Theory for Atomic Systems in a Strong DC Electric Field. In: Hotokka M, Brändas E, Maruani J, Delgado-Barrio G (eds) Advances in Quantum Methods and Applications in Chemistry, Physics, and Biology. Series: Progress in Theoretical Chemistry and Physics, vol 27 Springer, Cham, pp 161-177.
57. Glushkov AV (2019) Multiphoton Spectroscopy of Atoms and Nuclei in a Laser Field: Relativistic Energy Approach and Radiation Atomic Lines Moments Method. Advances in Quantum Chemistry, Vol 78, Elsevier, Amsterdam, pp 253-285. https://doi.org/10.1016/bs.aiq.2018.06.004.
58. Glushkov AV, Ambrosov SV, Ignatenko AV, Korchevsky DA (2004) DC Strong Field Stark Effect for Non-hydrogenic Atoms: New Consistent Quantum Mechanical Approach. Int Journ Quant Chem 99(5): 936-939.
59. Glushkov AV, Loboda AV, Gurnitskaya EP, Svinarenko AA (2009) QED theory of radiation lines for atoms in strong laser field. Physica Scripta 135:014022.
60. Glushkov AV, Ambrosov SV, Loboda AV, Gurnitskaya EP, Prepelitsa GP (2005) Consistent QED approach to calculation of electron-collision excitation cross-sections and strengths: Ne-like ions. Int. Journ.Quant.Chem. 104(4):562-569.
61. Glushkov AV (1997) QED Theory of nonlinear interaction of the complex atomic systems with laser field. Multiphoton resonances. J. Techn. Phys 38(2):219-224.
62. Furnstahl R J (2004) Next generation relativistic models. In: G A Lalazissis, P Ring P, Vretenar D (eds) Extended Density Functionals in Nuclear StructurePhysics, vol 641. Springer, Berlin, pp 1-30
63. Mohr PJ (1982) Self-energy of the n = 2 states in a strong Coulomb field. Phys Rev A 26:2338.
64. Drake G.W (1993) High precision calculations and QED effects for two-and three-electron atoms. Phys Scripta 46:116-124.

65. Johnson WR, Safronova MS, Safronova UI (2003) Combined effect of coherent Z exchange and hyperfine interaction in parity-nonconserving interaction. Phys Rev A 67:P062106.
66. Johnson WR, Sapistein J, Blundell SA (1993) Atomic structure calculations associated with PNC experiments in atomic caesium. Phys Scripta 46:184-192.
67. Flambaum VV, Ginges JS (2005) Radiative potential and calculations of QED radiative corrections to energy levels and electromagnetic amplitudes in many-electron atoms. Phys Rev A 72:052115.
68. Nagasawa T, Haga A, Nakano M (2004) Hyperfine splitting of hydrogenlike atoms based on relativistic mean field theory. Phys Rev C 2004 69:P034322:1-10.
69. Tomaselli M, Schneider SM, Kankeleit E et al (1995) Ground state magnetization of ^{209}Bi in a dynamic-correlation model. Phys Rev C 51(6):2989-2997.
70. Ahmad I, Dunfird RW, Esbensen H, Gemmell DS, Kanter EP, Run U, Siuthwirth SH (2000) Nuclear excitation by electron transition in ^{189}Os. Phys Rev 61:P051304.
71. Basar G, Basar Go, Acar G, Ozturk IK, Kroger S (2003) Hyperfine structure investigations of MnI: Experimental and theoretical studies of hyperfine structure in the even configurations. Phys Scripta 67:476-484.
72. Benczer-Koller N (2005) The role of magnetic moments in the determination of nuclear wave functions of short-lived excited states. J Phys CS 20:51-58.
73. Bieron J, Froese-Fischer C, Fritzsche S, Pachucki K (2004) Lifetime and hyperfine structure of $^3D_2$ state of radium. J Phys B: At Mol Opt Phys 37:L305-311.
74. Safronova MS, Johnson WR, Derevianko A (1999) Relativistic many-body calculations of energy levels, hyperfine constants, electric-dipole matrix elements, and static polarizabilities for alkali-metal atoms. Phys Rev A 60:P044103.
75. Safronova MS, Rupsi P, Jiang D et al (2009) New directions in atomic PNC. Nucl Phys A 827: 411-413.
76. Glushkov A V, Ambrosov S V, Loboda A V, Chernyakova Yu, Svinarenko A A , Khetselius O Yu (2004) QED calculation of the superheavy elements ions: energy levels, radiative corrections, and hfs for different nuclear models. Nucl. Phys. A.: nucl. and hadr. Phys. 734:21

77. Sukharev D E, Khetselius O Yu, Dubrovskaya Y V (2009) Sensing strong interaction effects in spectroscopy of hadronic atoms. Sensor Electr. and Microsyst. Techn. N3:16-21.
78. Glushkov AV, Khetselius OYu, Malinovskaya SV (2008) Optics and spectroscopy of cooperative laser-electron nuclear processes in atomic and molecular systems – new trend in quantum optics. Europ Phys Journ ST 160:195-204.
79. Glushkov A V, Ivanov L N, Letokhov V S (1991) Nuclear quantum optics. Preprint of Institute of Spectroscopy, USSR Academy of Sciences, Troitsk N4.
80. Chernyakova YuG, Vitavetskaya LA, Bashkaryov PG, Serga IN, Berestenko AG (2015) The radiative vacuum polarization contribution to the energy shift of some levels of the pionic hydrogen Photoelectronics 24:108-111.
81. Kuznetsova AA, Vitavetskaya LA, Chernyakova YG, Korchevsky DA (2013) Calculating the radiative vacuum polarization contribution to the energy shift of 2p-2s transition in pionic deuterium. Photoelectronics 22:122-127.
82. Glushkov AV, Khetselius OYu, Svinarenko AA (2013) Theoretical spectroscopy of autoionization resonances in spectra of lanthanide atoms. Phys Scr T153:014029.
83. Glushkov AV, Khetselius OYu, Svinarenko AA, IgnatenkoBuyadzhi VV, Ternovsky VB, Kuznetsova AA, Bashkarev PG (2017) Relativistic Perturbation Theory Formalism to Computing Spectra and Radiation Characteristics: Application to Heavy Element. In: Dimo I (ed) Recent Studies in Perturbation Theory. InTech, Uzunov, pp 131-150. https://doi.org/: 10.5772/intechopen.69102.
84. Svinarenko AA (2014) Study of spectra for lanthanides atoms with relativistic many-body perturbation theory: Rydberg resonances. J Phys: Conf Ser 548:012039.
85. Svinarenko AA, Glushkov AV, Khetselius OYu, Ternovsky VB, Dubrovskaya YuV, Kuznetsova AA, Buyadzhi VV (2017) Theoretical Spectroscopy of Rare-Earth Elements: Spectra and Autoionization Resonance. In: Jose EA (ed) Rare Earth Element. InTech, Orjuela, pp 83-104. https://doi.org/10.5772/intechopen.69314.
86. Glushkov AV, Butenko YuV, Serbov NG, Ambrosov SV, Orlova VE, Orlov SV, Balan AK, Dormostuchenko GM (1996) Calculation and extrapolation

of oscillator strengths in Rb-like, multiply charged ions. Russian Phys Journ 39(1):81-83.
87. Glushkov AV (1992) Oscillator strengths of Cs and Rb-like ions. Journal of Appl Spectroscopy 56(1):5-9.
88. Glushkov AV, Khetselius OYu, Lopatkin YM, Florko TA, Kovalenko OA, Mansarliysky VF (2014) Collisional shift of hyperfine line for rubidium in an atmosphere of the buffer inert gas. J of Phys: Conf Ser 548:012026.
89. Glushkov A, Malinovskaya S, Chernyakova Yu, Svinarenko A (2004) Cooperative Laser-Electron-Nuclear Processes: QED Calculation of Electron Satellites Spectra for Multi-Charged Ion in Laser Field. Int Journ Quant Chem 99(5):889-893.
90. Glushkov AV, Malinovskaya SV, Filatov VV (1989) S-Matrix formalism calculation of atomic transition probabilities with inclusion of polarization effects. Sov Phys Journal 32(12):1010-1014.
91. Glushkov AV, Svinarenko AA, Ignatenko AV (2011) Spectroscopy of autoionization resonances in spectra of the lanthanides atoms. Photoelectronics 20:90-94.
92. Glushkov AV (1990) Relativistic polarization potential of a many-electron atom. Sov Phys Journal 33(1):1-4.
93. Khetselius OYu (2015) Optimized Perturbation Theory for Calculating the Hyperfine Line Shift and Broadening of Heavy Atoms in a Buffer Gas. In: Nascimento M, Maruani J, Brändas E, Delgado-Barrio G (eds) Frontiers in Quantum Methods and Applications in Chemistry and Physics. Series: Progress in Theoretical Chemistry and Physics, vol. 29. Springer, Cham, pp. 55-76.
94. Khetselius OYu, Zaichko PA, Smirnov AV, Buyadzhi VV, Ternovsky VB, Florko TA, Mansarliysky VF (2017) Relativistic Many-Body Perturbation Theory Calculations of the Hyperfine Structure and Oscillator Strength Parameters for Some Heavy Element Atoms and Ions. In: Tadjer A, Pavlov R, Maruani J, Brändas E, Delgado-Barrio G (eds) Quantum Systems in Physics, Chemistry, and Biology. Series: Progress in Theoretical Chemistry and Physics, vol 30. Springer, Cham, pp 271-281.
95. Malinovskaya SV, Glushkov AV, Khetselius OYu, Svinarenko AA, Mischenko EV, Florko TA (2009) Optimized perturbation theory scheme for calculating the interatomic potentials and hyperfine lines shift for heavy atoms in the buffer inert gas. Int Journ Quant Chem 109:3325-3329.
96. Glushkov AV, Khetselius OY, Malinovskaya SV (2008) Molec Phys

106:1257-1260; https://doi.org/10.1080/00268970802158262
97. Glushkov AV, Malinovskaya SV, Khetselius OY, Loboda AV (2009) Monte-Carlo Quantum Chemistry of Biogene Amines. Laser and Neutron Capture Effects. AIP Conf Proc 1102:175-177; https://doi.org/10.1063/1.3108371
98. Glushkov AV, Khetselius OY, Loboda AV, Ignatenko A, Svinarenko A, Korchevsky D, Lovett L (2008) QED approach to modeling spectra of the multicharged ions in a plasma: Oscillator and electron-ion collision strengths. AIP Conf Proc 1058:175-177; https://doi.org/10.1063/1.3026437
99. Glushkov AV, Khetselius OYu, Kruglyak YuA, Ternovsky VB (2014) Calculational Methods in Quantum Geometry and Chaos theory. P.3. OSENU (TEC), Odessa.
100. Glushkov AV, Malinovskaya SV, Loboda AV, Shpinareva IM, Prepelitsa GP (2006) Consistent quantum approach to new laser-electron-nuclear effects in diatomic molecules. J Phys: Conf 35:420-424.
101. Glushkov AV, Malinovskaya SV, Loboda AV, Shpinareva IM, Gurnitskaya EP, Korchevsky DA (2005) Diagnostics of the collisionally pumped plasma and search of the optimal plasma parameters of x-ray lasing: Calculation of electron-collision strengths and rate coefficients for Ne-like plasma. J Phys: Conf Ser 11:188-198.
102. Malinovskaya SV, Glushkov AV, Khetselius OYu (2008) New laser-electron nuclear effects in the nuclear γ transition spectra in atomic and molecular systems. In: Wilson S, Grout PJ, Maruani J, Delgado-Barrio G, Piecuch P (eds) Frontiers in Quantum Systems in Chemistry and Physics. Series: Progress in Theoretical Chemistry and Physics, vol 18. Springer, Dordrecht, pp 525-541; https://doi.org/10.1007/978-1-4020-8707-3_24
103. Glushkov AV (1994) Calculation of parameters of the interaction potential between excited alkali atoms and mercury atoms-the Cs-, Fr-Hg interaction. Opt. and Spectr 77(1):5-10.
104. Glushkov AV New form of effective potential to calculate polarization effects of theπ-electronic states of organic molecules. (1994) J Struct Chem 34(5):659–665; https://doi.org/10.1007/BF00753565
105. Khetselius O Yu (2013) Forecasting evolutionary dynamics of chaotic systems using advanced non-linear prediction method. In: Dynamical Systems Applications, Eds. J Awrejcewicz, M Kazmierczak, P Olejnik, J Mrozowski (Lodz Univ.) T2:145-152.

106. Glushkov AV, Khetselius OYu, Svinarenko AA, Buyadzhi VV (2015) Spectroscopy of autoionization states of heavy atoms and multiply charged ions. TEC, Odessa.
107. Glushkov AV, Khetselius OYu, Svinarenko AA, Buyadzhi VV (2015) Methods of computational mathematics and mathematical physics. P.1. TES, Odessa.
108. Glushkov AV (2012) Methods of a Chaos Theory. Astroprint, Odessa
109. Hotokka M, Brändas E, Maruani J, Delgado-Barrio G (1.eds) Advances in Quantum Methods and Applications in Chemistry, Physics, and Biology. Series: Progress in Theoretical Chemistry and Physics, vol. 27. Springer, Cham, pp 161-177.
110. Glushkov AV, Malinovskaya SV, Loboda AV, Shpinareva IM, Gurnitskaya EP, Korchevsky DA (2005) Diagnostics of the collisionally pumped plasma and search of the optimal plasma parameters of x-ray lasing: Calculation of electron-collision strengths and rate coefficients for Ne-like plasma. J Phys: Conf Ser 11:188-198.
111. Glushkov AV, Malinovskaya SV, Chernyakova YuG, Svinarenko AA (2004) Cooperative Laser-Electron-Nuclear Processes: QED Calculation of Electron Satellites Spectra for Multi-Charged Ion in Laser Field. Int Journ Quant Chem 99(1.5):889-893.
112. Glushkov AV, Ambrosov SV, Ignatenko AV, Korchevsky DA (1.2004) DC Strong Field Stark Effect for Non-hydrogenic Atoms: New Consistent Quantum Mechanical Approach. Int Journ Quant Chem. 99:936-939.
113. Glushkov AV, Malinovskaya SV, Loboda AV, Shpinareva IM, Prepelitsa GP (2006) Consistent quantum approach to new laser-electron-nuclear effects in diatomic molecules. J Phys: Conf Ser. 35:420-424.
114. Glushkov AV, Kondratenko PA, Buyadgi VV, Kvasikova AS, Sakun TN, Shakhman AN (2014) Spectroscopy of cooperative laser electron-γ-nuclear processes in polyatomic molecules. J Phys: Conf Ser 548:012025.
115. Malinovskay S.V, Glushkov AV (1992) Calculation of the spectra of potassium-like multicharged ions. Russian Phys Journal. 35:999-1004.
116. Glushkov AV, Butenko YuV, Serbov NG, Ambrosov SV, Orlova VE, Orlov SV, Balan AK, Dormostuchenko GM (1.1996) Calculation of the oscillator strengths in Fr-like multiply charged ions. Journ of Applied Spectrosc 63:28-30.

117. Buyadzhi VV, Glushkov AV, Lovett L (2014) Spectroscopy of atoms and nuclei in a strong laser field: AC Stark effect and multiphoton resonances. Photoelectronics 23:38-43.
118. Glushkov AV, Kondratenko PA, Lepikh YaI, Fedchuk AP, Svinarenko AA, Lovett L (2009) Electrodynamical and quantum-chemical approaches to modelling the electrochemical ancatalytic processes on metals, metal alloys and semiconductors. Int Journ Quant Chem 109(14):3473-3481.
119. Florko TA, Ambrosov SV, Svinarenko AA, Tkach TB (2012) Collisional shift of the heavy atoms hyperfine lines in an atmosphere of the inert gas. J Phys: Conf Ser 397:012037.
120. Glushkov AV (1992) Negative ions of inert gases. JETP Lett 55(2):97-100.
121. Glushkov AV, Malinovskaya SV, Prepelitsa GP, Ignatenko VM (2005) Manifestation of the new laser-electron nuclear spectral effects in the thermalized plasma: QED theory of co-operative laser-electron-nuclear processes. J Phys: Conf Ser 11:199-206.
122. Glushkov AV (1988) True effective molecular valency hamiltonian in a logical semiempricial theory. Journal of Structural Chem 29(4):495-501.
123. Glushkov AV (1990) Correction for exchange and correlation effects in multielectron system theory. Journ of Struct Chem 31(4):529-532.
124. Glushkov AV, Efimov VA, Gopchenko ED, Dan'kov SV, Polishchyuk VN, Goloshchak OP (1998) calculation of spectroscopic characteristics 4 of alkali-metal dimers on the basis of a model perturbation theory. Optics and Spectr 84(5):670-678.
125. Buyadzhi VV (2015) Laser multiphoton spectroscopy of atom embedded in Debye plasmas: multiphoton resonances and transitions. Photoelectronics 24:128-133.
126. Glushkov AV, Ambrosov SV, Loboda AV, Gurnitskaya EP, Prepelitsa GP (2005) Consistent QED approach to calculation of electron-collision excitation cross-sections and strengths: Ne-like ions. Int Journ Quant Chem 104(4):562–569.
127. Svinarenko AA, Nikola LV, Prepelitsa GP, Tkach TB, Mischenk EV (2010) The Auger (1.autoionization) decay of excited states in spectra of multicharged ions: Relativistic theory. AIP Conf Proc 1290: 94-98.
128. Glushkov AV, Svinarenko AA, Ignatenko AV (2011) Spectroscopy of autoionization resonances in spectra of the lanthanides atoms. Photoelectronics 20:90-94.

129. Glushkov AV, Ambrosov SV, Ignatenko AV (2001) Non-hydrogenic atoms and Wannier-Mott excitons in a DC electric field: Photoionization, Stark effect, Resonances in continuum and Stochasticity. Photoelectronics 10:103-106.
130. Khetselius O Yu (2019) Optimized Relativistic Many-Body Perturbation Theory Calculation of Wavelengths and Oscillator Strengths for Li-like Multicharged Ions. Adv Quantum Chem, vol 78. Elsevier, Amsterdam, pp 223-251. https://doi.org/10.1016/bs.aiq.2018.06.001
131. Glushkov A.V., Multiphoton Spectroscopy of Atoms and Nuclei in a Laser Field: Relativistic Energy Approach and Radiation Atomic Lines Moments Method Adv Quantum Chem, vol 78. Elsevier, Amsterdam, pp 253-285. https://doi.org/10.1016/bs.aiq.2018.06.004
132. Malinovskaya SV, Dubrovskaya YuV, Zelentzova TN (2004) The atomic chemical environment effect on the β decay probabilities: Relativistic calculation. Herald of Kiev Nat Univ Ser: Phys-Math 4:427-432.
133. Buyadzhi VV, Zaichko PA, Antoshkina OA, Kulakli TA, Prepelitsa GP, Ternovsky VB, Mansarliysky VF (2017) Computing of radiation parameters for atoms and multicharged ions within relativistic energy approach: Advanced Code. J Phys: Conf Ser 905:012003.
134. Glushkov AV, Khetselius OYu, Svinarenko AA, Buyadzhi VV (2015) Spectroscopy of autoionization states of heavy atoms and multiply charged ions. TEC, Odessa.
135. Glushkov AV, Lovett L, Khetselius O, Gurnitskaya E, Dubrovskaya Y., Loboda AV (2009) Generalized multiconfiguration model of decay of multipole giant resonances applied to analysis of reaction (mu-n) on the nucleus 40Ca. Int. Journ. of Modern Phys. A 24(2-3):611-615.
136. Khetselius, O.Yu. (2010) Relativistic Hyperfine Structure Spectral Lines and Atomic Parity Non-conservation Effect in Heavy Atomic Systems within QED Theory. AIP Conf. Proceedings. 1290(1): 29-32.
137. Khetselius, O.Yu. Optimized Perturbation Theory for Calculating the Hyperfine Line Shift and Broadening of Heavy Atoms in a Buffer Gas. In Frontiers in Quantum Methods and Applications in Chemistry and Physics, Series: Progress in Theoretical Chemistry and Physics; Nascimento, M., Maruani, J., Brändas, E., Delgado-Barrio, G., Eds.; Springer: Cham, 2015; Vol. 29, pp. 55-76.
138. Svinarenko, A.A. (2014) Study of spectra for lanthanides atoms with relativistic many- body perturbation theory: Rydberg resonances. J. Phys.: Conf.

Ser. 548: 012039
139. Florko, T.A.; Ambrosov, S.V.; Svinarenko, A.A.; Tkach, T.B. (2012) Collisional shift of the heavy atoms hyperfine lines in an atmosphere of the inert gas. J. Phys.: Conf. Ser. 397: 012037.
140. Svinarenko, A.A.; Ignatenko, A.V.; Ternovsky, V.B.; Nikola, L.V.; Seredenko, S.S.; Tkach, T.B. (2014) Advanced relativistic model potential approach to calculation of radiation transition parameters in spectra of multicharged ions. J. Phys.: Conf. Ser. 548: 012047.
141. Serot, B.; Walecka, J. (1986) The Relativistic Nuclear Many Body Problem. In Adv. Nucl. Phys., Vol 16; Plenum Press: New York.
142. Bohr, O.; Motelsson, B. (1971) Structure of Atomic Nucleus; Plenum: New York.
143. Nagasawa, T.; Naga, A.; Nakano, M. (2004) Hyperfine splitting of hydrogen like atoms based on relativistic mean field theory, Phys. Rev. C 69: 034322.
144. Tittonen, I.; Lippmaa, M.; Ikonen, E.; Lindén, J.; Katil, T. (1992) Observation of Mössbauer resonance line splitting caused by Rabi oscillations. Phys. Rev. Lett. 69: 2815-2819.
145. Olariu, S.; Sinor, T.W.; Collins, C.B. (1994) Evidence for nuclear multiphoton transitions in ^{57}Fe based on radio-frequency sidebands to the forbidden hyperfine components of the 14.4-keV transition. Phys. Rev. B. 50: 616-618.
146. Buyadzhi, V.V.; Zaichko, P.A.; Gurskaya, M.Y.; Kuznetsova, A.A.; Ponomarenko, E.L.; Ternovsky, V.B. (2017) Relativistic theory of excitation and ionization of Rydberg atomic systems in a Black-body radiation field. J. Phys.: Conf. Ser. 810: 012047.
147. Buyadzhi, V.V.; Zaichko, P.A.; Antoshkina, O.A.; Kulakli,T.A.; Prepelitsa, G.P.; Ternovsky, V.B.; Mansarliysky, V.F. (2017) Computing of radiation parameters for atoms and multicharged ions within relativistic energy approach: Advanced Code. J. Phys.: Conf. Ser. 905: 012002.
148. Glushkov, A.V.; Rusov, V.D.; Ambrosov, S.V.; Loboda, A.V. (2002) Resonance states of compound super-heavy nucleus and EPPP in heavy nucleus collisions In New Projects and New Lines of Research in Nuclear Physics; Fazio, G., Hanappe, F., Eds.; World Scientific: Singapore. 126-132.
149. Glushkov, A.V. (2005) Energy approach to resonance states of compound superheavy nucleus and EPPP in heavy nuclei collisions In Low Energy Antiproton Physics; Grzonka, D., Czyzykiewicz, R., Oelert,W., Rozek, T.,

Winter, P., Eds.; AIP: New York, AIP Conf. Proc. 796: 206-210.
150. Glushkov, A.V. (2007) Resonance phenomena in heavy nuclei collisions and structurization of the positron spectrum. In Meson-Nucleon Physics and the Structure of the Nucleon; Krewald, S.; Machner, H.; IKP: Juelich; SLAC eConf C070910 (Menlo Park, CA, USA) **2007**, 2, 132-138.
151. Glushkov, A.V. (2012) Spectroscopy of cooperative muon-gamma-nuclear processes: Energy and spectral parameters J. Phys.: Conf. Ser. 397: 012011.
152. Khetselius, O.Yu. (2019) Optimized Relativistic Many-Body Perturbation Theory Calculation of Wavelengths and Oscillator Strengths for Li-like Multicharged Ions. In Advances in Quantum Chemistry: Quantum Systems in Physics, Chemistry and Biology, Theory, Interpretation, and Results; Jenkins, S.; Kirk, S.R.; Maruani, J.; Brändas, E.; Elsevier: Amsterdam, 78, Ch.8.
153. Letokhov, V.S. (1979) Using lasers in Atomic, nuclear and molecular physics. In Apllication of Lasers in Atomic, Nuclear and Molecular Physics, Prokhorov, A.M. and Letokhov, V.S., Eds.; Nauka: Moscow, pp 405-414.
154. Ivanov, L.N.; Letokhov, V.S. (1986) The splitting of excited electronic states in optically inactive molecules due to the parity-violating electron-nuclear interaction. J. Chem. Phys. 106: 6045-6050.
155. Glushkov, A.V. (2005) Atom in an electromagnetic field. KNT: Kiev.
156. Khetselius, O.Yu. (2008) Hyperfine structure of atomic spectra. Astroprint: Odessa
157. Buyadzhi, V.V. (2015) Laser multiphoton spectroscopy of atom embedded in Debye plasmas: multiphoton resonances and transitions. Photoelectronics. 24: 128-132.
158. Buyadzhi, V.V.; Chernyakova, Yu.G.; Smirnov, A.V.; Tkach, T.B. (2016) Electron-collisional spectroscopy of atoms and ions in plasma: Be-like ions. Photoelectronics. 25: 97-101.
159. Buyadzhi, V.V.; Chernyakova, Yu.G.; Antoshkina, O.A.; Tkach, T.B. (2017) Spectroscopy of multicharged ions in plasmas: Oscillator strengths of Be-like ion Fe. Photoelectronics. 26: 94-102.
160. Dalgarno, A.; Lewis, J.T. (1955) The exact calculation of long-range forces between atoms by perturbation theory. Proc. R. Soc. London Ser. A.233: 70-74
161. Mossman, S.; Lytel, R.; Kuzyk, M.G. (2016) Dalgarno–Lewis perturbation theory for nonlinear optics. J. Opt. Soc. Amer. B. 33: E31-E39.
162. Khetselius, O.Yu. (2011) Quantum structure of electroweak interaction in

heavy finite Fermi-systems. Astroprint: Odessa.
163. Blomqvist, J.; Wahlborn, S. (1960) Shell model calculations in the lead region with a diffuse nuclear potential. Arkiv för fysik. 16: 545-555;
164. Vennink, R.; Glaudemans, P.W.M. (1980) The shell model and collective structures in ^{54,55,56}Fe. Z. Phys. A. 294:241-252.
165. Glushkov A.V., Malinovskaya S.V., Sukharev D.E., Khetselius O.Yu., Loboda A.V., Lovett L. (2009) Green's function method in quantum chemistry: New numerical algorithm for the Dirac equation with complex energy and Fermi-model nuclear potential. Int. J. Quant. Chem. 109(8):1717-1727.
166. Khetselius O.Y., Ternovsky V.B., Dubrovskaya Y.V., and Svinarenko A. (2021) Electron-β-Nuclear Spectroscopy of Atomic Systems and Many-Body Perturbation Theory Approach to computing β-Decay Parameters In: Glushkov A.V., Khetselius O.Y., Maruani J., Brändas E. (Eds) Advances in Methods and Applications of Quantum Systems in Chemistry, Physics, and Biology, Ser.: Progress in Theoretical Chemistry and Physics, Cham: Springer. 33: 59-89.
167. Khetselius O.Y., Ternovsky V.B., Serga I., Svinarenko A (2021) Relativistic Quantum Chemistry and Spectroscopy of Some Kaonic Atoms: Hyperfine and Strong-Interaction Effects In: Glushkov A.V., Khetselius O.Y., Maruani J., Brändas E. (Eds) Advances in Methods and Applications of Quantum Systems in Chemistry, Physics, and Biology, Ser.: Progress in Theoretical Chemistry and Physics, Cham: Springer. 33: 91-110.
168. Glushkov A.V., Ignatenko A.V., Tsudik A.V., Mykhailov A.L. (2021) A Quasiparticle Fermi-Liquid Density Functional Approach to Atomic and Diatomic Systems. Spectroscopic factors In: Glushkov A.V., Khetselius O.Y., Maruani J., Brändas E. (Eds) Advances in Methods and Applications of Quantum Systems in Chemistry, Physics, and Biology, Ser.: Progress in Theoretical Chemistry and Physics, Cham: Springer. 33: 133-150.
169. Glushkov A.V., Ternovsky E.V., Mansarliysky V.F., Zaichko P.A. (2021) Advanced Quantum Approach to the Calculation of Probabilities of Cooperative Electronic-Vibrational-Nuclear Transitions in Spectra of Diatomic Molecules. In: Glushkov A.V., Khetselius O.Y., Maruani J., Brändas E. (Eds) Advances in Methods and Applications of Quantum Systems in Chemistry, Physics, and Biology, Cham: Springer. 33: 181-206.
170. Glushkov A.V., Khetselius O., Buyadzhi V. (2018) Atom in a laser field and laser separation of radioactive isotopes. TES: Odessa.

Навчальне електронне видання

GLUSHKOV Alexander V. and KHETSELIUS Olga Yu.

АТОМНА ОПТИКА ТА СПЕКТРОСКОПІЯ. Ч.5

Конспект лекцій
(англійською мовою)

Видавець і виготовлювач
Одеський державний екологічний університет
вул. Львівська, 15, м. Одеса, 65016
тел./факс: (0482) 32-67-35
E-mail: info@odeku.edu.ua
Свідоцтво суб'єкта видавничої справи
ДК № 5242 від 08.11.2016